AIMS Mathematics, 10(1): 1704–1740.
DOI: 10.3934/math.2025078
Received: 29 September 2024
Revised: 14 December 2024
Accepted: 16 January 2025
Published: 24 January 2025

https://www.aimspress.com/journal/Math

Research article

Solving fuzzy system of Fredholm integro-differential equations of the second kind by using homotopy analysis method

Zena Talal Yassin[1,*], Waleed Al-Hayani[1], Ali F. Jameel[2], Ala Amourah[2,3,*] and Nidal Anakira[2]

[1] Department of Mathematics, College of Computer Science and Mathematics, University of Mosul, Iraq
[2] Mathematics Education Program, Faculty of Education and Arts, Sohar University, Sohar 311, Oman
[3] Applied Science Private University, Amman, Jordan

* **Correspondence:** Email: zena-talal@uomosul.edu.iq, AAmourah@su.edu.om.

Abstract: Certain phenomena with uncertain properties that take the shape of intricate mathematical modeling are known to have fuzzy system integro-differential equations (FSIDEs). The methods used to roughly solve FSIDEs seek to provide open-form solutions that are regarded as solutions for polynomial series. However, for many FSIDEs, the polynomial series solutions are not easily derived, especially in nonlinear forms. Meanwhile, some existing approximate techniques cannot guarantee convergence of the series solution. Nevertheless, to solve second-kind fuzzy Fredholm integro-differential equations (FFSIDEs), there exist perturbation techniques based on the standard Homotopy Analysis Method (HAM) that have the ability to control and rate solution convergence. Therefore, this study focused on modifying new approximate techniques, fuzzy Fredholm HAM (HAMFF), for solving second-kind FFSIDEs subject to initial and boundary value problems. In the theoretical framework modification, the establishment of the series solution convergence was done based on combining some fuzzy sets theory concepts and convergence-control parameters from standard HAM. The HAMFF was not only able to solve linear systems but also difficult nonlinear systems with proper accuracy. The demonstration of the modified technique's performance was shown in comparison to other methods, where HAMFF was individually superior in terms of accuracy for solving linear and nonlinear test problems of FFSIDEs.

Keywords: fuzzy sets theory; fuzzy system of Fredholm integro-differential equations (FSFIDEs); homotopy analysis method (HAM); convergent control parameter
Mathematics Subject Classification: 35A15, 45G15, 65H20, 49M27

1. Introduction

The mathematical models with uncertainty properties take the forms fuzzy differential equations (FDEs), fuzzy integral equations (FIEs), or fuzzy integro-differential equations (FIDEs). Therefore, the solution of integro-differential equations (IDEs) that have been considered the main core of some physical systems play a significant role in science and engineering [1–6]. Some of these systems are linear and nonlinear Fredholm IDEs, and their solutions are continuously growing in many physical problems that arise naturally under uncertainty properties. The study of FDEs and fuzzy integral equations is currently the focus of much research. The starting point of fuzzy sets was first introduced by Zadeh [7]. The fuzzy integral equations were previously derived by Kaleva and Seikkala [8,9]. Lately, a lot of academics have focused on this topic and produced a ton of studies that are published in the literature [10]. As a result, fuzzy models constrained by FSIDEs behave more like the actual process because the after effect is incorporated into it by using the concepts of fuzzy derivatives and fuzzy integrals [11–12], which have several benefits, including the ability to incorporate additional conditions into the problem structure and the ability to structure realistic problems. However, the idea of Hukuhara derivatives that FDEs were developed [13]. FDEs and FIEs were extended to FIDEs, which first appeared in 1999 [14]. That study paved the way for future research on FSIDEs by applying principles from fuzzy sets theory to the analysis of FDEs and FIEs.

Typically, it is difficult and limiting to obtain the exact analytical solutions for linear FIDEs. Unfortunately, there isn't an analytical solution for the majority of the intricate physical phenomena that can be explained by nonlinear FSIDEs [15]. Analytical solutions are not found in many cases. However, there is always a need for the solutions to these equations because of their practical applications, such as the fuzzy Riccati differential equation [16]. Therefore, in order to handle such fuzzy situations, it is frequently important to suggest effective approximate techniques. In the meantime, the approximate-analytic class of methods under the approximation techniques can directly evaluate the solution accuracy for the systems involving high-order FIDEs. In addition to being applicable to nonlinear systems of FIDEs without the need for linearization or discretization as numerical approximate techniques [17]. Although some numerical class techniques and approximate analytical class techniques are employed and analyzed to obtain the approximate solution of a system of second-kind Fredholm-integro differential equations in the crisp domain [8–12], also in the fuzzy domain, the learning algorithm approximate method (LAM) is used to obtain the solution of these systems in 2017 [12].

Nevertheless, the series solution's convergence cannot be guaranteed by some current approximate-analytical techniques. However, perturbation-based methods such as the standard fuzzy HAM approach [17] exist to solve fuzzy problems and have the capacity to control convergence. The idea of HAM first appeared in Liao PhD thesis 1992 [18] to deal with approximate solutions for linear and nonlinear mathematical engineering models. It was found that the HAM provides a solution in series form with a degree of polynomial function HAM that converges to the close form solution; otherwise, the solution is approximated to some degree of accuracy to the open form solution [17,19]. Also, the basic idea of HAM provides a great technique to rate the solution convergence through the convergence control parameter. The standard HAM has been modified and used to solve a variety of mathematical problems in the fuzzy domain, such as fuzzy FDEs [19], fuzzy partial differential equations [20], fuzzy fractional differential equations [21,22], fuzzy integral equations [17], and fuzzy integro-differential equations [23]. According to the aforementioned survey, the majority of the

research that used numerical and approximation analytical techniques was applied on crisp system Fredholm IDEs, with only one implementation on FFSIDEs. As a result, we believe it is vital to propose new approximation analytical techniques to overcome such challenges, as we will demonstrate in the next sections. HAMFF, would give significant contribution toward overcoming obstacles of existing methods such as the Variational iteration method (VIM), the Adomian decomposition method (ADM) etc for example the proposed methods will help us to simplify the complexity of the uncertain nonlocal derivative when solving FFSIDEs. Furthermore, unlike all existing methods HAMFF provides the convergence parameter to control the accuracy of the solution, thus ensuring the convergence of the approximate series solutions. Also, the series solutions provided by the HAMFF have the ability to show the graphical designs of the solutions. Consequently, the goal of this research is to create a new convergence-controlled approximate analytical technique, HAMFF, for solving problems that are subject to boundary and initial conditions. The formulation and analysis of this study involving a theoretical framework and methodology relies on some well-known concepts of fuzzy sets theory that have been used to help build our recommended technique to solve FFSIDEs. These concepts include properties of fuzzy numbers [24], fuzzy extension principles [25], the α-cuts [26], fuzzy function [27], fuzzy differentiations, and the context of fuzzy integration [28–30].

2. Fuzzy analysis of FSFIDEs

The following terms must be defined in order to analyze the suggested system in this work.

Definition 2.1. [24] A triangular fuzzy number is a fuzzy set $\tilde{A} = (s_1, s_2, s_3)$ that, satisfies the membership function,

$$Tri_{\tilde{A}}(x) = \begin{cases} 0 & \text{if} \quad x < s_1 \\ (x - s_1)/(s_2 - s_1) & \text{if} \quad s_1 \le x \le s_2 \\ (s_3 - x)/(s_3 - s_2) & \text{if} \quad s_2 \le x \le s_3 \\ 0 & \text{if} \quad x > s_3 \end{cases},$$

where the crisp interval can be defined by α-cut operation where $\alpha \in [0,1]$, such that,

$$\tilde{A}_\alpha = \left[{s_1}^{(\alpha)}, {s_3}^{(\alpha)}\right] = [(s_2 - s_1)\alpha + s_1, -(s_3 - s_2)\alpha + a_3]$$

where at $\alpha = 1$ the lower and upper bound of $\tilde{A}_\alpha$ are equal and this is the original crisp number.

Moreover, according to [24] the triangular fuzzy number satisfies the following properties:

(1) It is convex (the line by α-cut is continuous and the α-cut interval satisfies for $A_\alpha = \left[{s_1}^{(\alpha)}, {s_3}^{(\alpha)}\right]$, if there is two different $s_1 < s_2 \Rightarrow {s_1}^{(\alpha_1)} \le {s_1}^{(\alpha_2)}$ and ${s_3}^{(\alpha_1)} \ge {s_3}^{(\alpha_2)}$).
(2) It is normalized (the maximum membership value is 1, $\exists x \in \mathbb{R}, \mu_A(x) = 1$).
(3) Its membership function is piecewise continuous.
(4) It is defined in the real number.

Definition 2.2. [28] The integral of the fuzzy function $\tilde{f}$ in $[a, b]$ is the fuzzy number with α-levels denoted by,

$$\left[\int_a^b \tilde{f}(x)dx\right]^\alpha = \left[\int_a^b \underline{f}(x;\alpha)dx\,, \int_a^b \bar{f}(x;\alpha)dx\right]$$

where $\int_a^b \underline{f}(x;\alpha)dx$ and $\int_a^b \bar{f}(x;\alpha)dx$ are the Riemann integrals of the real functions $\underline{f}(x;\alpha)$, $\underline{f}(x;\alpha)$in the interval $[a,b]$.

Now, the general form of the fuzzy system of Fredholm integro-differential equations (FSFIDEs) of the second kind [10] is defined as

$$\tilde{u}_i^{(n)}(x,\alpha) = \tilde{f}_i(x,\alpha) + \sum_{j=1}^{2} \tilde{\lambda}_{ij}(\alpha) \int_a^b \tilde{k}_{ij}\big(x,t,\tilde{u}_i(t,\alpha)\big), \quad i = 1,2 \tag{1}$$

the initial conditions

$$\tilde{u}_i(0,\alpha) = \Big(\underline{a}_i(\alpha), \bar{a}_i(\alpha)\Big), \tilde{u}_i'(0,\alpha) = \Big(\underline{a}_i'(\alpha), \bar{a}_i'(\alpha)\Big), \dots, \tilde{u}_i^{(n-1)}(0,\alpha) = \Big(\underline{a}_i^{(n-1)}(\alpha), \bar{a}_i^{(n-1)}(\alpha)\Big)$$

where $0 \le \alpha \le 1$, $\tilde{\lambda}_{ij}$ are positive fuzzy parameters, $\tilde{k}_{ij}$ is an arbitrary fuzzy function called the kernal of integral and $\tilde{f}_i(x,\alpha)$ is the given fuzzy function of $x \in [a,b]$ with $\tilde{u}_i(x,\alpha)$ as the unknown fuzzy functions

$$\tilde{u}_i(x,\alpha) = \big[\underline{u}_i(x,\alpha), \bar{u}_i(x,\alpha)\big],$$
$$\tilde{f}_i(x,\alpha) = \Big[\underline{f}_i(x,\alpha), \bar{f}_i(x,\alpha)\Big],$$

then we can write Eq (1) as

$$\underline{u}_i^{(n)}(x,\alpha) = \underline{f}_i(x,\alpha) + \sum_{j=1}^{2} \underline{\lambda}_{ij}(\alpha) \int_a^b \underline{k}_{ij}\Big(x,t,\underline{u}_i(t,\alpha)\Big)\,dt,$$
$$\bar{u}_i^{(n)}(x,\alpha) = \bar{f}_i(x,\alpha) + \sum_{j=1}^{2} \bar{\lambda}_{ij}(\alpha) \int_a^b \bar{k}_{ij}\big(x,t,\bar{u}_i(t,\alpha)\big)dt.$$

3. Formulation and analysis of HAMFF

For the analysis of HAM in [18], we can have the substantive of the solution of Eq (1) for all α-level sets values where $\alpha \in [0,1]$ is the following process.
The zeroth-order deformation is

$$(1-q)L\big[\tilde{u}_i(x,q,\alpha) - \tilde{f}_i(x,\alpha)\big] q\tilde{h}H(t)N_i[\tilde{u}_i(x,q,\alpha)], \tag{2}$$

and by taking $q = 0$ and $q = 1$ we get.

$$\left.\begin{aligned} \tilde{u}_i(x,0,\alpha) &= \tilde{f}_i(x,\alpha) \\ \tilde{u}_i(x,1,\alpha) &= \tilde{u}_i(x,\alpha) \end{aligned}\right\}. \tag{3}$$

From Eq (2), the fuzzy initial guess $\tilde{u}_{i,0}(x,\alpha)$ can be determined from $\tilde{f}_i(x,\alpha)$, then the taylor series

of q for $\tilde{u}_i(x,q,\alpha)$ is

$$\tilde{u}_i(x,q,\alpha) = \tilde{u}_i(x,0,\alpha) + \sum_{m=1}^{\infty} \frac{\tilde{u}_{i,m}\left(x,\alpha,\tilde{h}(x)\right)}{m!} q^m, \tag{4}$$

where

$$\tilde{u}_{i,m}\left(x,\alpha,\tilde{h}(\alpha)\right) = \frac{1}{m!} \frac{\partial \tilde{u}_{i,m}\left(x,\alpha,q,\tilde{h}(\alpha)\right)}{\partial q^m}\Big|_{q=0} \tag{5}$$

the m-th order deformation f or $q=1$ in Eq (4) is as follows;

$$L\left[\tilde{u}_{i,m}(x,\alpha) - \chi_m \tilde{u}_{i,m-1}(x,\alpha)\right] = \tilde{h}(\alpha)\left[R_{i,m}\left(\vec{\tilde{u}}_{i,m-1}\right)\right],$$

$$R_{i,m}\left(\vec{\tilde{u}}_{i,m-1}\right) = \tilde{u}^n{}_{i,m-1} - (1-\chi_m)\tilde{f}_i(x,\alpha) - \sum_{j=1}^{2} \tilde{\lambda}_{ij}(\alpha) \int_a^b \tilde{F}_{ij}\left(\tilde{u}_{i,m-1}(t,\alpha)\right) dt,$$

and the series solution of Eq (1) takes the following forms

$$\begin{cases} \underline{u}_{i,0}(x,\alpha) + \sum_{m=1}^{\infty} \underline{u}_{i,m}(x,\alpha,\underline{h}(\alpha)) \\ \bar{u}_{i,0}(x,\alpha) + \sum_{m=1}^{\infty} \bar{u}_{i,m}(x,\alpha,\bar{h}(\alpha)) \end{cases}. \tag{6}$$

A convenient selecting of $\tilde{h}(\alpha)$ obtains the convergence of Eq (6) therefore, the solution in series form (homotopy solution).

4. Convergence analysis HAMFF

The approximate solution of Eq (1) is convergence based on best values of the parameter $\tilde{h}(\alpha)$ therefore, $\tilde{h}(\alpha)$ should be discussed to supply enough accuracy for ascertain order of the HAMFF series solution. Therefore, an accurate convergent solution is guaranteed when the convergence parameter is chosen appropriately. Finding the approximate solution with the least amount of residual error is one common method for choosing $\tilde{h}(\alpha)$. Assume that the residual of Eq (6) is denoted by $\widetilde{RE} = \left[\underline{RE}, \overline{RE}\right]$, then defined the following residual form

$$\widetilde{RE}_1\left(x,\alpha,\tilde{h}_1(\alpha)\right) = \tilde{u}^{(n)}\left(x,\alpha,\tilde{h}_1(\alpha)\right) - \tilde{f}_1(x,\alpha) - \tilde{\lambda}_1(x) \int_a^b \tilde{k}_1\left(x,t,\tilde{u}\left(t,\alpha,\tilde{h}_1(x)\right)\right),$$
$$\widetilde{RE}_2\left(x,\alpha,\tilde{h}_2(\alpha)\right) = \tilde{v}^{(n)}\left(x,\alpha,\tilde{h}_2(\alpha)\right) - \tilde{f}_2(x,\alpha) - \tilde{\lambda}_2(\alpha) \int_a^b \tilde{k}_2\left(x,t,\tilde{v}\left(t,\alpha,\tilde{h}_2(\alpha)\right)\right),$$

the mean square residual error (MSRE) of Eq (6) is define in the following form:

$$\widetilde{MSRE}_i\left(x,\alpha,\tilde{h}_i(\alpha)\right) = \sqrt{\frac{\sum_{j=0}^{10}\left(\widetilde{RE}_i(x,0.1j,\tilde{h}_i(\alpha))\right)^2}{10+1}}, \; i=1,2, \; 0<\alpha\leq 1, \tag{7}$$

by using the least square method to optimize the values of $\tilde{h}_i(\alpha)$ such that

$$J_i\left(x,\alpha,\tilde{h}_i(\alpha)\right)=\left(\int_0^1 \widetilde{MSRE}_i\left(x,\alpha,\tilde{h}_i(\alpha)\right)\right)^2 dx,\ i=1,2 \tag{8}$$

and the nonlinear equation coming from Eq. (8) for any $\alpha\in(0,1]$ is derived such that

$$\frac{\partial \tilde{J}_i\left(x,\alpha,\tilde{h}_i(\alpha)\right)}{\partial \tilde{h}_i(\alpha)}=0\Rightarrow\begin{cases}\dfrac{\partial \underline{J}_i(x,\alpha,h_i(\alpha))}{\partial h_i(x)}=0,\\ \dfrac{\partial \bar{J}_i\left(x,\alpha,\bar{h}_i(\alpha)\right)}{\partial \bar{h}_i'(\alpha)}=0.\end{cases}$$

Finally, the equation is solved for $\tilde{h}_i(\alpha)$ in each α-level set to obtain the best value of $\tilde{h}$ by plotting curves called h-curves such that horizontal line segment with respect to $\tilde{u}_i^{(n)}(x,\alpha)$ to illustrate the best region of the $\tilde{h}(\alpha)$values, which are the for $x_0<x<X$. It is familiar in the fuzzy environment to display the contract h-curves, and to find the optimal value $\tilde{h}(\alpha)$ for each $\alpha\in[0,1]$. The choice the best value of $\tilde{h}(\alpha)$ provides the best accurate solution of the FFSIDEs with its corresponding fuzzy level set $\tilde{\alpha}=\left[\underline{\alpha},\overline{\alpha}\right]$, and then applied $\underline{\alpha}$ for each lower level set gets the best lower approximate solution. A similar step is applied to $\overline{\alpha}$ to determine the best upper solution. The following algorithm is summarizing the dynamic convergence of HAMFF:

Step 1: Set $\tilde{u}_{i,0}(x,\alpha)=\tilde{u}_{i,0},\left(\tilde{u}_{i,0}=\left\{\underline{u}_{i,0},\bar{u}_{i,0}\right\}\right),\tilde{u}_i{}'(0,\alpha)=\left(\underline{a}_i{}'(\alpha),\bar{a}_i{}'(\alpha)\right),\ldots..,\tilde{u}_i{}^{(n-1)}(0,\alpha)=\left(\underline{a}_i{}^{(n-1)}(\alpha),\bar{a}_i{}^{(n-1)}(\alpha)\right)$.

Step 2: Set $\tilde{\lambda}(\alpha)=\left[\underline{\lambda}(\alpha),\bar{\lambda}(\alpha)\right]$.

Step 3: Set $m=1,2,3,\ldots,n$.

Step 4: Set $m=m+1$ and for $m=1$ to $m<n$ evaluate

$$\tilde{x}_{i,m}(x,\alpha)=\tilde{x}_{i,m-1}^{\mathrm{n}}(\mathrm{x},\alpha)+\tilde{h}(\alpha)\ \left[\tilde{x}_{i,m-1}^{\mathrm{n}}(x,\alpha)-\int_a^b \tilde{k}_{ij}\left(x,t,\tilde{x}_{im-1}\left(x,\alpha,\tilde{h}(\alpha)\right)dt-(1-\chi_m)\tilde{f}_i(x,\alpha)\right].$$

Step 5: Compute

$$\tilde{x}_{i,m}\left(\mathrm{x},\alpha,\tilde{h}(\alpha)\right)=\tilde{x}_{0,m-1}(\mathrm{x},\alpha)+\sum_{k=1}^{n}\tilde{x}_{k,m-1}(\mathrm{x},\alpha),\ i=1,2.$$

Step 6: Set the value of $\alpha_0\in[0,1],x\in[a,b]$ and evaluate

$$\tilde{h}(\alpha_0)=\frac{\partial\tilde{x}\left(x,\alpha_0,\tilde{h}(\alpha_0)\right)}{\partial\tilde{h}(\alpha_0)},$$

then plot the h-curve.

Step 7: Define the residual form in Eqs (6)–(8) and substitute the $\tilde{h}(\alpha_0)$ in Eq (9) to compute the optimal value of $\tilde{h}(\alpha_0)$.

Step 8: Replace-again the optimal values of $\tilde{h}(\alpha)$ for the lower and upper levels in Eq (10).

5. Applications and numerical results

In this section, the HAMFF is applied to achieve an approximate-exact solution for FSFIDEs in three problems. We defined the maximum errors as follows to demonstrate the high accuracy of the solution when compared with the exact solution.

$\|\cdot\|_\infty = \|\tilde{u}_E(x,\alpha) - \tilde{u}(x,\alpha)\|_\infty$,
where:
$\tilde{u}_E(x,\alpha)$: Fuzzy exact solution,
$\tilde{u}(x,\alpha)$: Fuzzy approximate solution (HAM).
Moreover, giving the residual error (RE), the computation associated with the problem were performed using the Maple 18 package with a precision of 30 digits.

Problem 1. Consider the following the crisp second kind linear SFIDEs [10]

$$\begin{aligned} u''(x) - xv(x) - u(x) &= (x-2)\sin x \\ &\quad + \int_0^1 x[\cos t\, u(t) - \sin t\, v(t)]dt\,, \\ v''(x) - 2xu'(x) + v(x) &= -2x\cos x \\ &\quad + \int_0^1 \sin x\,[cos\, t\, u(t) - sin\, t\, v(t)]dt. \end{aligned} \tag{9}$$

Subject to initial conditions (ICs).

$$\begin{aligned} &u(0) = 0,\ u'(0) = 1, \\ &\tilde{v}(0) = 1,\ v'(0,\alpha) = 0. \end{aligned} \tag{10}$$

Since this problem is crisp SFIDEs, we will first present fuzzification of the equation. In this study, the fuzzy version of system (9) is created. Such that from Definition 2.2 the fuzzy version of the integral operator is follows:

$$\int_0^1 x[\cos t\, \tilde{u}(t,\alpha) - \sin t\, \tilde{v}(t,\alpha)]dt = \begin{cases} \int_0^1 x\left[\cos t\, \underline{u}(t,\alpha) - \sin t\, \underline{v}(t,\alpha)\right]dt \\ \int_0^1 x[\cos t\, \overline{u}(t,\alpha) - \sin t\, \overline{v}(t,\alpha)]dt \end{cases}$$

$$\int_0^1 \sin x\,[cos\, t\, \tilde{u}(t,\alpha) - sin\, t\, \tilde{v}(t,\alpha)]dt = \begin{cases} \int_0^1 \sin x\left[cos\, t\, \underline{u}(t,\alpha) - sin\, t\, \underline{v}(t,\alpha)\right]dt \\ \int_0^1 \sin x\,[cos\, t\, \overline{u}(t,\alpha) - sin\, t\, \overline{v}(t,\alpha)]dt. \end{cases}$$

Now according to the fuzzy analysis in [17] the fuzzy version of system (9) is as follows:

$$\begin{aligned} \tilde{u}''(x,\alpha) - x\tilde{v}(x,\alpha) - \tilde{u}(x,\alpha) &= (x-2)\sin x \\ &\quad + \int_0^1 x[\cos t\, \tilde{u}(t,\alpha) - \sin t\, \tilde{v}(t,\alpha)]dt\,, \\ \tilde{v}''(x,\alpha) - 2x\widetilde{u'}(x,\alpha) + \tilde{v}(x,\alpha) &= -2x\cos x \\ &\quad + \int_0^1 \sin x\,[cos\, t\, \tilde{u}(t,\alpha) - sin\, t\, \tilde{v}(t,\alpha)]dt. \end{aligned} \tag{11}$$

From the Definition 2.1 of the triangular fuzzy numbers, we can defuzzify the ICs. Let $\left[\tilde{0}\right]_\alpha$ and $\left[\tilde{1}\right]_\alpha$ be triangular fuzzy numbers corresponding with the ICs (10) for all $\alpha \in [0,1]$ such that

$$\tilde{u}(0,\alpha) = \left[\tilde{0}\right]_\alpha = (-1,0,1),\ \tilde{u}'(0,\alpha) = \left[\tilde{1}\right]_\alpha = (3,4,5)$$

$$\tilde{v}(0,\alpha) = \left[\tilde{1}\right]_\alpha = \left(\frac{1}{4},\frac{3}{4},\frac{7}{4}\right),\ \tilde{v}'^{(0,\alpha)} = \left[\tilde{0}\right]_\alpha = \left(-\frac{1}{2},0,\frac{1}{2}\right).$$

According to the α-cut of triangular fuzzy number in Definition 2.1 the following fuzzy ICs of system (11) are defined as follows

$$\begin{aligned} &\tilde{u}(0,\alpha) = (\alpha-1,1-\alpha),\ \tilde{u}'(0,\alpha) = (4\alpha-3,5-4\alpha),\\ &\tilde{v}(0,\alpha) = \left(\frac{3}{4}\alpha+\frac{1}{4},\frac{7}{4}-\frac{3}{4}\alpha\right),\ \tilde{v}'(0,\alpha) = \left(\frac{1}{2}\alpha-\frac{1}{2},\frac{1}{2}-\frac{1}{2}\alpha\right), \end{aligned} \tag{12}$$

where $\tilde{f}_1(x,\alpha) = \left[\underline{f_1}(x,\alpha),\overline{f}_1(x,\alpha)\right]$ and $\tilde{f}_2(x,\alpha) = \left[\underline{f_2}(x,\alpha),\overline{f}_2(x,\alpha)\right]$ are given by

$$\begin{aligned} \underline{f_1}(x,\alpha) = {} & (0.708073418x - 3.\sin(x) + 3.5\sin(x)\,x)\alpha - 0.708073418x + \sin(x)\\ & - 2.5\,sin(x)\,x, \end{aligned}$$

$$\underline{f_2}(x,\alpha) = (0.708073418sin(x) - 3.0cos(x)x)\alpha - 0.708073418sin(x) + cos(x)x,$$

$$\begin{aligned} \overline{f}_1(x,\alpha) = {} & (-0.708073418x + 3.sin(x) - 3.5sin(x)x)\alpha + 0.708073418x - 5.0sin(x)\\ & + 4.5sin(x)x, \end{aligned}$$

$$\overline{f}_2(x,\alpha) = (-0.708073418sin(x) + 3.0cos(x)x)\alpha + 0.708073418sin(x) - 5.0cos(x)x.$$

The exact solutions of the system (11) are

$$\begin{aligned} \tilde{u}_E(x,\alpha) &= \left[\alpha x - \frac{1}{6}\alpha x^3 + \frac{1}{120}\alpha x^5, (2-\alpha)x - \left(\frac{1}{3}-\frac{1}{6}\alpha\right)x^3 + \left(\frac{1}{60}-\frac{1}{120}\alpha\right)x^5\right],\\ \tilde{v}_E(x,\alpha) &= \left[(2\alpha-1) - \frac{1}{2}\alpha x^2 + \frac{1}{24}\alpha x^4, (3-2\alpha) - \left(1-\frac{1}{2}\alpha\right)x^2 + \left(\frac{1}{12}-\frac{1}{24}\alpha\right)x^4\right]. \end{aligned} \tag{14}$$

To solve the fuzzy system (11) according to the ICs (12) by means of the HAMFF to obtain the initial approximations. from section 3, the iterations of HAMFF are determined in the following recursive way:

$$\begin{aligned} \tilde{u}_0(x,\alpha) &= \tilde{u}(0,\alpha) + x\tilde{u}'(0,\alpha),\\ \tilde{v}_0(x,\alpha) &= \tilde{v}(0,\alpha) + x\tilde{v}'(0,\alpha), \end{aligned} \tag{15}$$

and choosing the linear operators

$$\begin{aligned} L[\tilde{u}(x,q,\alpha)] &= \frac{\partial^2\tilde{u}(x,q,\alpha)}{\partial^2 x},\\ L[\tilde{v}(x,q,\alpha)] &= \frac{\partial^2\tilde{v}(x,q,\alpha)}{\partial^2 x}, \end{aligned}\quad L^{-1} = \int_0^x\int_0^x(\cdot)dtdt, \tag{16}$$

with the property $L[c_1 + c_2x] = 0$, where c_1 and c_2 are constants. Furthermore, formulation of system (9) according to HAMFF in Section 3 involved the embedding parameter $q \in [0,1]$ and the parameter can be defined with the nonlinear operators as follows:

$$\begin{cases} N_1[\tilde{u}(x,q;\alpha),\tilde{v}(x,q;\alpha)] = \frac{\partial^2\tilde{u}(x,q;\alpha)}{\partial^2 x} - x\tilde{v}'(x,q;\alpha) - \tilde{u}(x,q;\alpha) \\ \quad -\tilde{f}_1(x,\alpha) - \int_0^1 x[(\cos t)\tilde{u}(t,q;\alpha) - (\sin t)\tilde{v}(t,q;\alpha)]dt\,, \\ N_2[\tilde{u}(x,q;\alpha),\tilde{v}(x,q;\alpha)] = \frac{\partial^2\tilde{v}(x,q,\alpha)}{\partial^2 x} - 2x\tilde{u}'(x,q;\alpha) + \tilde{v}(x,q;\alpha) \\ \quad +\tilde{f}_2(x,\alpha) - \int_0^1 \sin x\,[(\cos t)\tilde{u}(t,q;\alpha) - (\sin t)\tilde{v}(t,q;\alpha)]dt\,. \end{cases} \tag{17}$$

Using the above definition, with the assumption $H(x) = 1$ we construct the zeroth-order deformation equation

$$\begin{cases} (1-q)L[\tilde{u}(x,q,\alpha) - \tilde{u}_0(x,\alpha)] = qhH(x)N_1[\tilde{u}(x,q;\alpha),\tilde{v}(x,q;\alpha)], \\ (1-q)L[\tilde{v}(x,q,\alpha) - \tilde{v}_0(x,\alpha)] = qhH(x)N_2[\tilde{u}(x,q;\alpha),\tilde{v}(x,q;\alpha)]. \end{cases} \tag{18}$$

Obviously, when $q = 0$ and $q = 1$

$$\tilde{u}(x,0,\alpha) = \tilde{u}_0(x,\alpha), \quad \tilde{u}(x,1,\alpha) = \tilde{u}(x,\alpha),$$
$$\tilde{v}(x,0,\alpha) = \tilde{v}_0(x,\alpha), \quad \tilde{v}(x,1,\alpha) = \tilde{v}(x,\alpha).$$

Thus, we obtain the $mth-$order deformation equations for $m \geq 1$ which are

$$\begin{cases} L[\tilde{u}_m(x,\alpha) - \chi_m\tilde{u}_{m-1}(x,\alpha)] = h\big[R_{1,m}\big(\tilde{\vec{u}}_{m-1},\tilde{\vec{v}}_{m-1}\big)\big], \\ L[\tilde{v}_m(x,\alpha) - \chi_m\tilde{v}_{m-1}(x,\alpha)] = h\big[R_{2,m}\big(\tilde{\vec{u}}_{m-1},\tilde{\vec{v}}_{m-1}\big)\big], \end{cases} \tag{19}$$

where

$$\begin{aligned} R_{1,m}\big(\tilde{\vec{u}}_{m-1},\tilde{\vec{v}}_{m-1}\big) &= \tilde{u}''_{m-1}(x,\alpha) - x\tilde{v}'_{m-1}(x,\alpha) - \tilde{u}_{m-1}(x,\alpha) \\ &\quad -(1-\chi_m)\tilde{f}_1(x,\alpha) - \lambda_1\int_0^1 x[\cos t\,\tilde{u}_{m-1}(t,\alpha) - \sin t\,\tilde{v}_{m-1}(t,\alpha)]dt\,, \\ R_{2,m}\big(\tilde{\vec{u}}_{m-1},\tilde{\vec{v}}_{m-1}\big) &= \tilde{v}''_{m-1}(x,\alpha) - 2x\tilde{u}'_{m-1}(x,\alpha) + \tilde{v}_{m-1}(x,\alpha) \\ &\quad +(1-\chi_m)\tilde{f}_2(x,\alpha) - \lambda_2\int_0^1 \sin x\,[\cos t\,\tilde{u}_{m-1}(t,\alpha) - \sin t\,\tilde{v}_{m-1}(t,\alpha)]dt\,. \end{aligned} \tag{20}$$

Now, for $m \geq 1$, the solutions of the *mth*-order deformation Eq (17) are

$$\begin{cases} \tilde{u}_m(x,\alpha) = \chi_m\tilde{u}_{m-1}(x,\alpha) + hL^{-1}\big[R_{1,m}\big(\tilde{\vec{u}}_{m-1},\tilde{\vec{v}}_{m-1}\big)\big], \\ \tilde{v}_m(x,\alpha) = \chi_m\tilde{v}_{m-1}(x,\alpha) + hL^{-1}\big[R_{2,m}\big(\tilde{\vec{u}}_{m-1},\tilde{\vec{v}}_{m-1}\big)\big]. \end{cases} \tag{21}$$

Thus, the approximate solutions in a series form are given by

$$\begin{aligned} \tilde{u}(x,\alpha) &= \tilde{u}_0(x,\alpha) + \textstyle\sum_{k=1}^{6}\tilde{u}_k(x,\alpha)\,, \\ \tilde{v}(x,\alpha) &= \tilde{v}_0(x,\alpha) + \textstyle\sum_{k=1}^{6}\tilde{v}_k(x,\alpha)\,. \end{aligned} \tag{22}$$

From Section 4, the residual function with respect to this solution for the system (9) is obtained by the substitution of the series solution (19) into the original system (9) such that

$$\begin{aligned}\widetilde{RE}_1(x,\alpha) &= \tilde{u}''(x,\alpha) - x\tilde{v}'(x,\alpha) - \tilde{u}(x,\alpha) - \tilde{f}_1(x,\alpha)\\ &\quad - \int_0^1 x[(\cos t)\tilde{u}(t,\alpha) - (\sin t)\tilde{v}(t,\alpha)]dt\,,\\ \widetilde{RE}_2(x,\alpha) &= \tilde{v}''(x,\alpha) - 2x\widetilde{u}'(x,\alpha) + \tilde{v}(x,\alpha) + \tilde{f}_2(x,\alpha)\\ &\quad - \int_0^1 \sin x\,[(\cos t)\tilde{u}(t,\alpha) - (\sin t)\tilde{v}(t,\alpha)]dt\,.\end{aligned} \tag{23}$$

The $\tilde{h}_i(\alpha)$-curves of sixth-order HAMFF upper and lower bound solutions $\tilde{u}(x,\alpha)$ and $\tilde{v}(x,\alpha)$ at $x = 0.3$ and $\alpha = 0.5$ for system (9) are shown in the following Tables 1 and 2 and Figures 1–4.

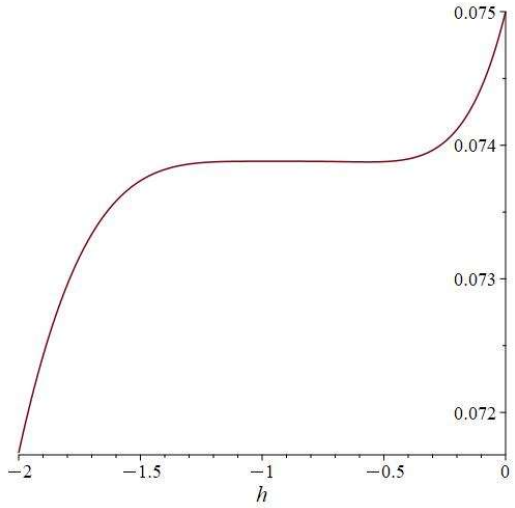

Figure 1. The h-curve representation of sixth-order HAMFF lower solution for system (9) of $\underline{u}(0.3; 0.5; h)$.

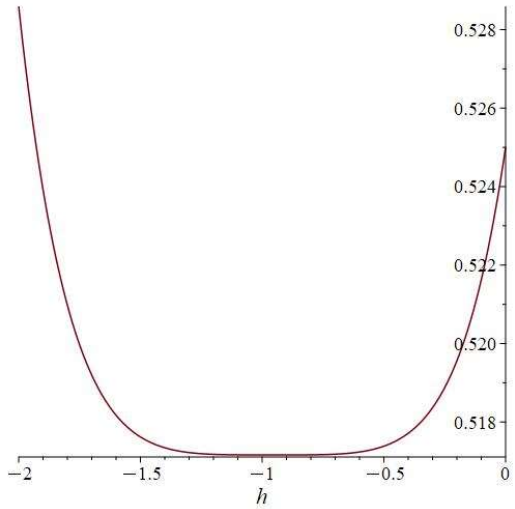

Figure 2. The h-curve representation of sixth-order HAMFF upper solution for system (11) of $\overline{u}(0.3; 0.5; h)$.

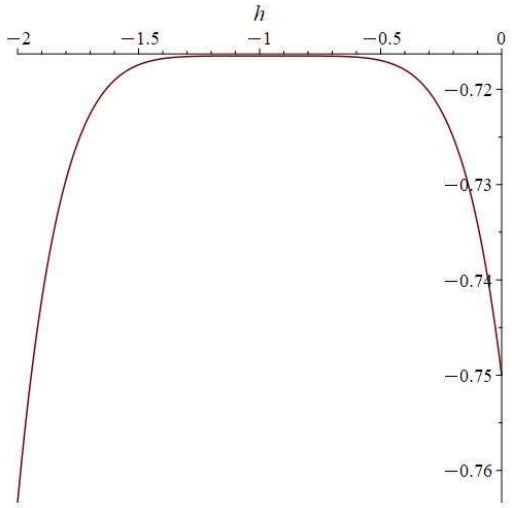

Figure 3. The h-curve representation of sixth-order HAMFF lower solution for system (11) of $\underline{v}(0.3; 0.5; h)$.

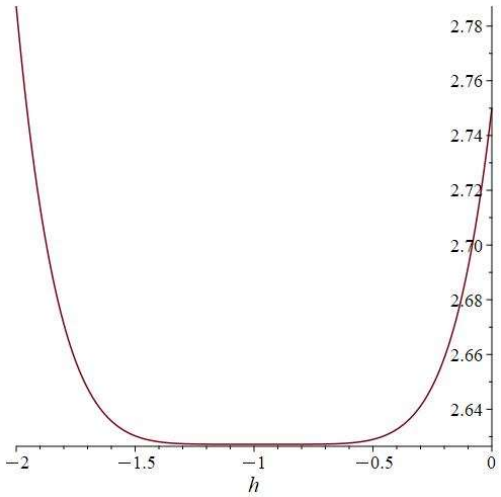

Figure 4. The h-curve representation of sixth-order HAMFF upper solution for system (9) of $\overline{v}(0.3; 0.5; h)$.

Table 1. Best values of the convergence control parameter of sixth-order HAMFF solution $\tilde{u}(x, \alpha)$ of system (11) at $x = 0.3$ and $\alpha = 0.5$, where * denoted to the optimal value of $\tilde{h}_1$.

$\underline{h}_{11}$*	-0.993770765902976	$\underline{h}_{12}$	-0.940282902800624	$\underline{h}_{13}$	-0.913774159351708
$\overline{h}_{11}$*	-0.995692236847504	$\overline{h}_{12}$	-0.937399868820798	$\overline{h}_{13}$	-0.908804197021662

Table 2. Best values of the convergence control parameter of sixth-order HAMFF solution $\tilde{v}(x,\alpha)$ of system (11) at $x = 0.3$ and $\alpha = 0.5$, where * denoted to the optimal value of $\tilde{h}_2$.

$\underline{h}_{21}$*	-0.997396591174385	$\underline{h}_{22}$	-0.943482345592162	$\underline{h}_{23}$	-0.911405157147745
$\overline{h}_{21}$*	-0.999232447779833	$\overline{h}_{22}$	-0.940161255064283	$\overline{h}_{23}$	-0.906821208973723

By comparing the Tables 3–6, we can see how the results improve after the minimization process.

Table 3. Solution and accuracy sixth-order HAMFF for system (9) of $\tilde{u}(x,\alpha)$ at $x = 0.5$ and $\tilde{h}_i = -1$ with $0 \le \alpha \le 1$.

α	$\underline{u}_E(x,\alpha)$	$\underline{u}(x,\alpha)$	$\lvert\underline{u}_E(x,\alpha) - \underline{u}(x,\alpha)\rvert$	$\overline{u}_E(x,\alpha)$	$\overline{u}(x,\alpha)$	$\lvert\overline{u}_E(x,\alpha) - \overline{u}(x,\alpha)\rvert$
0.0	-0.239712769	-0.239712815	4.628E-08	1.198563846	1.198563912	6.571E-08
0.2	-0.095885107	-0.095885142	3.508E-08	1.054736184	1.054736239	5.451E-08
0.4	0.047942553	0.047942529	2.388E-08	0.910908523	0.910908566	4.331E-08
0.6	0.191770215	0.191770202	1.268E-08	0.767080861	0.767080893	3.211E-08
0.8	0.335597877	0.335597875	1.485E-09	0.623253200	0.623253221	2.091E-08
1.0	0.479425538	0.479425548	9.714E-09	0.479425538	0.479425548	9.714E-09

Table 4. Solution and accuracy sixth-order HAMFF for system (11) of $\tilde{v}(x,\alpha)$ at $x = 0.5$ and $\tilde{h}_i = -1$ with $0 \le \alpha \le 1$.

α	$\underline{v}_E(x,\alpha)$	$\underline{v}(x,\alpha)$	$\lvert\underline{v}_E(x,\alpha) - \underline{v}(x,\alpha)\rvert$	$\overline{v}_E(x,\alpha)$	$\overline{v}(x,\alpha)$	$\lvert\overline{v}_E(x,\alpha) - \overline{v}(x,\alpha)\rvert$
0.0	-2.193956404	-2.193956432	2.793E-08	3.949121528	3.949121561	3.340E-08
0.2	-1.579648611	-1.579648633	2.180E-08	3.334813735	3.334813762	2.726E-08
0.4	-0.965340818	-0.965340833	1.566E-08	2.720505941	2.720505962	2.113E-08
0.6	-0.351033024	-0.351033034	9.535E-09	2.106198148	2.106198163	1.499E-08
0.8	0.263274768	0.263274765	3.401E-09	1.491890355	1.491890364	8.865E-09
1.0	0.877582561	0.877582564	2.731E-09	0.877582561	0.877582564	2.731E-09

Tables 3 and 4 show a comparison of the absolute errors applying the HAMFF $(m = 6)$ with the exact solutions (11) within the interval $0 \le \alpha \le 1$ at $x = 0.5$ with best values of the convergence control parameter $\tilde{h}_i$ after minimization which are listed in the following tables (see Tables 5 and 6).

Table 5. Solution and accuracy sixth-order HAMFF for system (11) of $\tilde{u}(x,\alpha)$ at $= 0.3$, $\tilde{h}_i = \underline{h}_{11}, \tilde{h}_i = \overline{h}_{11}$and $0 \le \alpha \le 1$.

α	$\underline{u}_E(x,\alpha)$	$\underline{u}(x,\alpha)$	$\lvert\underline{u}_E(x,\alpha) - \underline{u}(x,\alpha)\rvert$	$\overline{u}_E(x,\alpha)$	$\overline{u}(x,\alpha)$	$\lvert\overline{u}_E(x,\alpha) - \overline{u}(x,\alpha)\rvert$
0.0	-0.239712769	-0.239712775	5.966E-09	1.198563846	1.198563860	1.350E-08
0.2	-0.095885107	-0.095885113	6.133E-09	1.054736184	1.054736195	1.040E-08
0.4	0.047942553	0.047942547	6.300E-09	0.910908523	0.910908530	7.315E-09
0.6	0.191770215	0.191770208	6.467E-09	0.767080861	0.767080865	4.221E-09
0.8	0.335597877	0.335597870	6.634E-09	0.623253200	0.623253201	1.128E-09
1.0	0.479425538	0.479425531	6.800E-09	0.479425538	0.479425536	1.964E-09

Table 6. Solution and accuracy sixth-order HAMFF for system (11) of $\tilde{v}(x,\alpha)$ at $x = 0.3$, $\tilde{h}_i = \underline{h}_{21}$, $\tilde{h}_i = \overline{h}_{21}$and $0 \le \alpha \le 1$.

α	$\underline{v}_E(x,\alpha)$	$\underline{v}(x,\alpha)$	$\lvert\underline{v}_E(x,\alpha) - \underline{v}(x,\alpha)\rvert$	$\overline{v}_E(x,\alpha)$	$\overline{v}(x,\alpha)$	$\lvert\overline{v}_E(x,\alpha) - \overline{v}(x,\alpha)\rvert$
0.0	-2.193956404	-2.193956416	1.186E-08	3.949121528	3.949121552	2.445E-08
0.2	-1.579648611	-1.579648621	1.028E-08	3.334813735	3.334813754	1.970E-08
0.4	-0.965340818	-0.965340826	8.700E-09	2.720505941	2.720505956	1.496E-08
0.6	-0.351033024	-0.351033031	7.118E-09	2.106198148	2.106198158	1.021E-08
0.8	0.263274768	0.263274763	5.536E-09	1.491890355	1.491890360	5.463E-09
1.0	0.877582561	0.877582557	3.954E-09	0.877582561	0.877582562	7.146E-10

In the following Figures 5–10 shows the exact solutions ($\tilde{u}_E(x,\alpha)$, $\tilde{v}_E(x,\alpha)$) and the fuzzy approximate solutions by HAM ($\tilde{u}(x,\alpha)$, $\tilde{v}(x,\alpha)$) of the system (11) are in the form of fuzzy numbers for any $0 \le \alpha \le 1$ at $x = 0.3$ and $\tilde{h}_i = -1$.

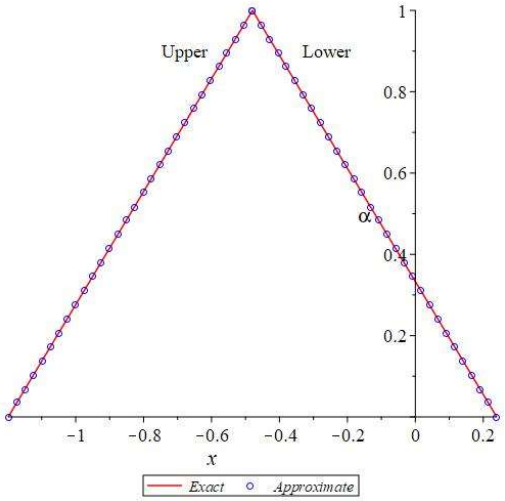

Figure 5. The exact and HAMFF lower and upper solutions of system (11) $\tilde{u}_E(x,\alpha)$ and $\tilde{u}(x,\alpha)$ for all $\alpha \in [0,1]$.

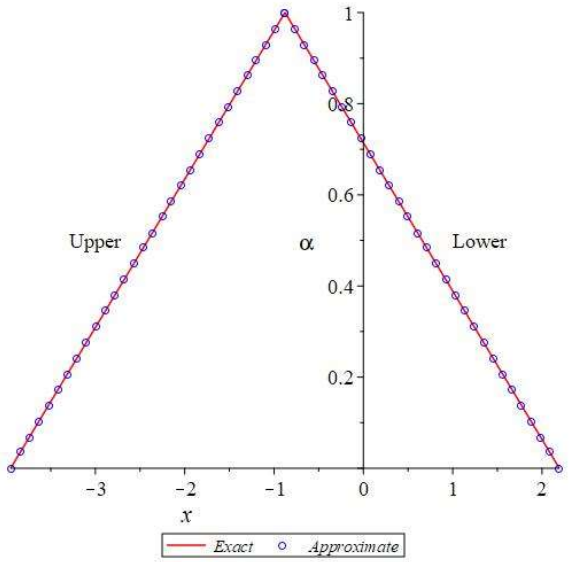

Figure 6. The exact and HAMFF lower and upper solutions of system (11) $\tilde{v}_E(x,\alpha)$ and $\tilde{v}(x,\alpha)$ for all $\alpha \in [0,1]$.

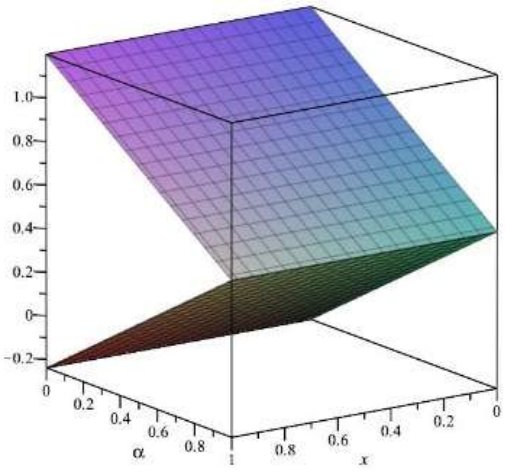

Figure 7. The exact lower and upper solutions of system (11) $\tilde{u}_E(x,\alpha)$ for all $x,\alpha \in [0,1]$.

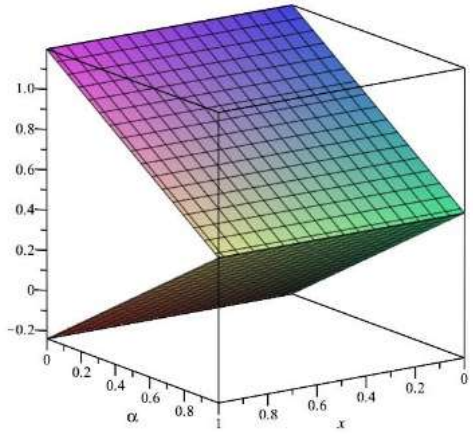

Figure 8. The HAMFF lower and upper solutions of system (11) and $\tilde{u}(x,\alpha)$ for all $x,\alpha \in [0,1]$.

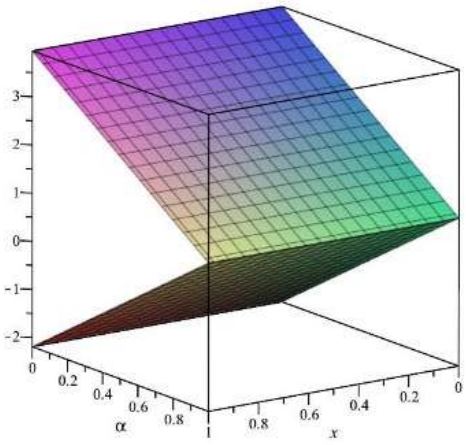

Figure 9. The exact lower and upper solutions of system (11) $\tilde{v}_E(x,\alpha)$ for all $x,\alpha \in [0,1]$.

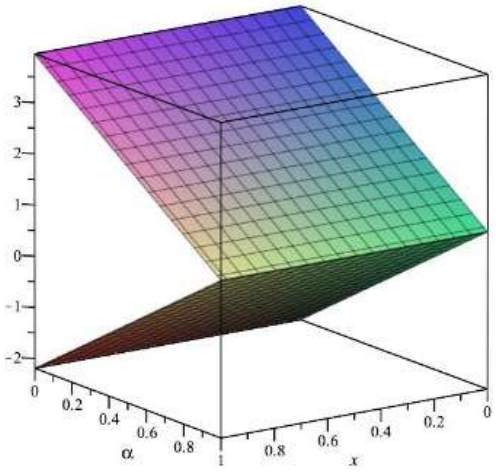

Figure 10. The HAMFF lower and upper solutions of system (9) and $\tilde{v}(x,\alpha)$ for all $x,\alpha \in [0,1]$.

According to Figures 5–10, one can summarize that the sixth-order HAMFF solutions of system (9) satisfied the fuzzy solution in triangular fuzzy number forms. To show HAMFF accuracy of Eq (11) crisp version was solved via the Euler polynomials (EP) [10] and Laguerre polynomials methods [11] (MLP), comparison between sixth-order HAMFF solution EP with $N = 6$ iterations MLP [11] with $N = 5$ iterations can be made when $\alpha = 1$ which is equivalent to the crisp version of Eq (11) at the same values of $x \in [0,1]$ that illustrated in Tables 7 and 8 and are displayed in Table 9 below.

Table 7. Accuracy of sixth-order HAMFF solution for system (11) at $\alpha = 1$ and $h_i = -1$.

x	$u_E(x,1)$	$u(x,1)$	$\lvert u_E(x,1) - u(x,1)\rvert$	$v_E(x,1)$	$v(x,1)$	$\lvert v_E(x,1) - v(x,1)\rvert$
0.0	0.0	0.0	0.0	1.0	1.0	0.0
0.2	0.198669330	0.198669332	1.832E-09	0.980066577	0.980066579	1.758E-09
0.4	0.389418342	0.389418351	8.876E-09	0.921060994	0.921061000	6.568E-09
0.6	0.564642473	0.564642474	7.133E-10	0.825335614	0.825335599	1.523E-08
0.8	0.717356090	0.717355970	1.199E-07	0.696706709	0.696706666	4.290E-08
1.0	0.841470984	0.841470265	7.190E-07	0.540302305	0.540305187	2.881E-06

Table 8. Control parameters at $\alpha = 1$, where h_i is the ideal expression.

h_{11}*	-0.997358653933643	h_{12}	-0.934546746098124	h_{13}	-0.905342473297271
h_{21}*	-1.000822093275177	h_{22}	-0.937048072427569	h_{23}	-0.903768109332694

Table 9. Accuracy of sixth-order HAMFF solution with EP [10] and MLP [11] for system (11) at $\alpha = 1$ and h_i with optimal values of $h_1 = \underline{h}_{11}$, $h_2 = \overline{h}_{21}$.

$\lvert u_E(x,1) - u(x,1)\rvert$	[10]	[11]	$\lvert v_E(x,1) - v(x,1)\rvert$	[10]	[11]
3.309E-07	5.801E-05	1.568E-06	2.941E-06	1.016E-04	5.780E-06

Indeed, the sixth- order HAMFF solution system (9) obtained better solution in terms of accuracy over EP [10] and MLP [11] at $\alpha = 1$ as illustrated in Table 9 above.

Problem 2. Consider the fuzzy version following second kind linear FSFIDEs as follows:

$$\begin{aligned}\tilde{u}''(x,\alpha) - x\tilde{v}'(x,\alpha) + 2x\tilde{u}(x,\alpha) &= 2 + \tfrac{320}{66}x - \tfrac{37}{12}x^2 + 2x^3 \\ &\quad + \textstyle\int_0^1 xt[x\tilde{u}(t,\alpha) - t\tilde{v}(t,\alpha)]dt, \\ \tilde{v}''(x,\alpha) - 2x\tilde{u}'(x,\alpha) + \tilde{v}(x,\alpha) &= -1 - \tfrac{109}{30}x - 5x^2 \\ &\quad + \textstyle\int_0^1 xt[\tilde{u}(t,\alpha) + t^2\tilde{v}(t,\alpha)]dt\,,\end{aligned} \tag{24}$$

with the boundary conditions (BCs)

$$\begin{aligned}\tilde{u}(0,\alpha) &= (2\alpha + 1{,}5 - 2\alpha),\ \tilde{u}(1,\alpha) = (3\alpha - 1{,}5 - 3\alpha), \\ \tilde{v}(0,\alpha) &= (2\alpha - 1{,}3 - 2\alpha),\ \tilde{v}(1,\alpha) = (6\alpha - 5{,}7 - 6\alpha).\end{aligned} \tag{25}$$

System (24) was derived utilizing the same fuzzy analysis in problem 1 from the crisp version SFIDEs in [11],

where

$\tilde{f}_1(x,\alpha) = \left[\underline{f}_1(x,\alpha), \overline{f}_1(x,\alpha)\right]$ and $\tilde{f}_2(x,\alpha) = \left[\underline{f}_2(x,\alpha), \overline{f}_2(x,\alpha)\right]$ are given by

$$\underline{f}_1(x,\alpha) = \left(\frac{91}{30}x - \frac{79}{12}x^2 + 2 + 2x^3\right)\alpha + \frac{47}{20}x + \frac{7}{2}x^2,$$

$$\underline{f}_2(x,\alpha) = \frac{23}{5}\alpha x - \frac{29}{30}x + 3\alpha - 4 - 3\alpha x^2 - 2x^2,$$

$$\overline{f}_1(x,\alpha)=\left(-\frac{91}{30}x+\frac{79}{12}x^2-2-2x^3\right)\alpha-\frac{29}{3}x^2+\frac{101}{12}x+4+4x^3,$$
$$\overline{f}_2(x,\alpha)=\left(-\frac{23}{5}x-3+3x^2\right)\alpha+\frac{247}{30}x-8x^2+2.$$

The exact solutions of the system (24) are

$$\tilde{u}_E(x,\alpha)=\left[\alpha\underline{x}^2-2\alpha\underline{x}+2\alpha+1,(2-\alpha)\overline{x}^2-(4-2\alpha)\overline{x}+(5-2\alpha)\right],$$
$$\tilde{v}_E(x,\alpha)=\left[(\alpha-2)\underline{x}^2+(2\alpha-1)\underline{x}+\alpha,-\alpha\overline{x}^2+(3-2\alpha)\overline{x}+(2-\alpha)\right].$$

To solve system (24) approximately, the HAMFF is applied to system (24) such that the method iterations are determined in the following recursive way:

$$\begin{aligned}\tilde{u}_0(x,\alpha)&=\tilde{u}(0,\alpha)+x\tilde{u}'(0,\alpha),\\ \tilde{v}_0(x,\alpha)&=\tilde{v}(0,\alpha)+x\tilde{v}'(0,\alpha),\end{aligned}\tag{26}$$

where $\tilde{u}'(0,\alpha)=\tilde{C}_1$, and $\tilde{v}'(0,\alpha)=\tilde{C}_2$, calculated from the BCs (25).

Choosing the linear operators

$$\begin{aligned}L[\tilde{u}(x,q,\alpha)]&=\frac{\partial^2\tilde{u}(x,q,\alpha)}{\partial^2 x},\\ L[\tilde{v}(x,q,\alpha)]&=\frac{\partial^2\tilde{v}(x,q,\alpha)}{\partial^2 x},\end{aligned}\quad L^{-1}=\int_0^x\int_0^x(\cdot)dtdt,\tag{27}$$

with the property $L[c_1+c_2x]=0$, where c_1 and c_2 are constants.

$\underline{C}_1=2.7581\times10^{-9}-1.999999995\alpha$, $\overline{C}_1=-3.999999989+1.999999995\alpha$,

$\underline{C}_2=-1.000000009+2.000000001\alpha$, $\overline{C}_2=2.999999992-2.000000001\alpha$.

As in Problem 1, nonlinear operators of system (21) are defined as follows

$$\begin{cases}N_1[\tilde{u}(x,q,\alpha),\tilde{v}(x,q,\alpha)]=\frac{\partial^2\tilde{\phi}_1(x,q,\alpha)}{\partial^2 x}-x\widetilde{v'}(x,q,\alpha)+(2x)\tilde{u}(x,q,\alpha)\\ \qquad -\tilde{f}_1(x,\alpha)-\int_0^1 xt[x\tilde{u}(x,q,\alpha)-t\tilde{v}(x,q,\alpha)]dt,\\ N_2[\tilde{u}(x,q,\alpha),\tilde{v}(x,q,\alpha)]=\frac{\partial^2\tilde{v}(x,q,\alpha)}{\partial^2 x}-2x\widetilde{u'}(x,q,\alpha)+\tilde{v}(x,q,\alpha)\\ \qquad +\tilde{f}_2(x,\alpha)-\int_0^1(xt)[\tilde{u}(x,q,\alpha)+t^2\tilde{v}(x,q,\alpha)]dt.\end{cases}\tag{28}$$

Using the above definition, with the assumption $H(x)=1$ we construct the zeroth-order deformation equation

$$\begin{cases}(1-q)L[\tilde{u}(x,q,\alpha)-\tilde{u}_0(x,\alpha)]=qhH(x)N_1[\tilde{u}(x,q,\alpha),\tilde{v}(x,q,\alpha)],\\ (1-q)L[\tilde{v}(x,q,\alpha)-\tilde{v}_0(x,\alpha)]=qhH(x)N_2[\tilde{u}(x,q,\alpha),\tilde{v}(x,q,\alpha)].\end{cases}\tag{29}$$

Obviously, when $q=0$ and $q=1$

$$\tilde{u}(x,0,\alpha)=\tilde{u}_0(x,\alpha),\quad \tilde{u}(x,1,\alpha)=\tilde{u}(x,\alpha),$$
$$\tilde{v}(x,0,\alpha)=\tilde{v}_0(x,\alpha),\quad \tilde{v}(x,1,\alpha)=\tilde{v}(x,\alpha).$$

Thus, we obtain the $mth-$order deformation equations for $m\geq1$ which are

$$\begin{cases}L[\tilde{u}_m(x,\alpha)-\chi_m\tilde{u}_{m-1}(x,\alpha)]=h\left[R_{1,m}\left(\vec{\tilde{u}}_{m-1},\vec{\tilde{v}}_{m-1}\right)\right],\\ L[\tilde{v}_m(x,\alpha)-\chi_m\tilde{v}_{m-1}(x,\alpha)]=h\left[R_{2,m}\left(\vec{\tilde{u}}_{m-1},\vec{\tilde{v}}_{m-1}\right)\right],\end{cases}\tag{30}$$

where

$$\begin{aligned} R_{1,m}\left(\tilde{\vec{u}}_{m-1}, \tilde{\vec{v}}_{m-1}\right) &= \tilde{v}''_{m-1}(x,\alpha) - x\tilde{v}'_{m-1}(x,\alpha) + 2x\tilde{u}_{m-1}(x,\alpha) \\ &-(1-\chi_m)\tilde{f}_1(x,\alpha) - \int_0^1 xt[x\tilde{u}_{m-1}(t,\alpha) - t\tilde{v}_{m-1}(t,\alpha)]dt\,, \\ R_{2,m}\left(\tilde{\vec{u}}_{m-1}, \tilde{\vec{v}}_{m-1}\right) &= +\tilde{v}''_{m-1}(x,\alpha) - 2x\tilde{u}'_{m-1}(x,\alpha) + \tilde{v}_{m-1}(x,\alpha) \\ &+(1-\chi_m)\tilde{f}_2(x,\alpha) - \int_0^1 xt[\tilde{u}_{m-1}(t,\alpha) + t^2\tilde{v}_{m-1}(t,\alpha)]dt\,. \end{aligned} \tag{31}$$

Now, for $m \geq 1$, the solutions of the *mth*-order deformation system (24) are

$$\begin{cases} \tilde{u}_m(x,\alpha) = \chi_m\tilde{u}_{m-1}(x,\alpha) + hL^{-1}\left[R_{1,m}\left(\tilde{\vec{u}}_{m-1}, \tilde{\vec{v}}_{m-1}\right)\right], \\ \tilde{v}_m(x,\alpha) = \chi_m\tilde{v}_{m-1}(x,\alpha) + hL^{-1}\left[R_{2,m}\left(\tilde{\vec{u}}_{m-1}, \tilde{\vec{v}}_{m-1}\right)\right]. \end{cases} \tag{32}$$

Thus, the approximate solutions in a series form are given by

$$\begin{aligned} \tilde{u}(x,\alpha) &= \tilde{u}_0(x,\alpha) + \sum_{k=1}^{9}\tilde{u}_k(x,\alpha)\,, \\ \tilde{v}(x,\alpha) &= \tilde{v}_0(x,\alpha) + \sum_{k=1}^{9}\tilde{v}_k(x,\alpha)\,. \end{aligned} \tag{33}$$

The residual error function with respect to this solution for the system (21) is

$$\begin{aligned} \widetilde{RE}_1(x,\alpha) &= \tilde{u}''(x,\alpha) - x\tilde{v}'(x,\alpha) + 2x\tilde{u}(x,\alpha) - \tilde{f}_1(x,\alpha) - \int_0^1 xt[x\tilde{u}(t,\alpha) - t\tilde{v}(t,\alpha)]dt\,, \\ \widetilde{RE}_2(x,\alpha) &= \tilde{v}''(x,\alpha) - 2x\widetilde{u'}(x,\alpha) + \tilde{v}(x,\alpha) - \tilde{f}_2(x,\alpha) - \int_0^1 xt[\tilde{u}(t,\alpha) + t^2\tilde{v}(t,\alpha)]dt\,. \end{aligned} \tag{34}$$

The $\tilde{h}_i(\alpha)$-curves of ninth-order HAMFF upper and lower bound solutions $\tilde{u}(x,\alpha)$ and $\tilde{v}(x,\alpha)$ at $x = 0.1$ and $\alpha = 0.5$ for system (21) are shown in the following Tables 10 and 11 and Figures 11–14.

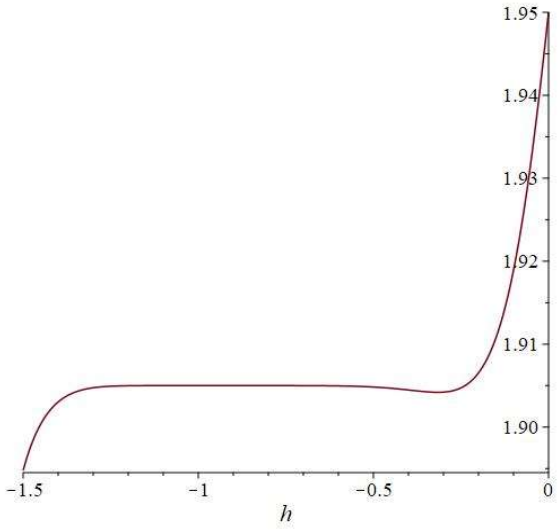

Figure 11. The h-curve representation of ninth-order HAMFF lower solution for system (24) of $\underline{u}(0.1; 0.5; h)$.

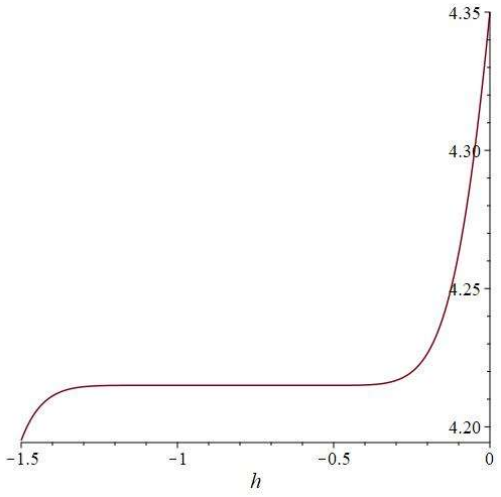

Figure 12. The h-curve representation of ninth-order HAMFF upper solution for system (24) of $\overline{u}(0.1; 0.5; h)$.

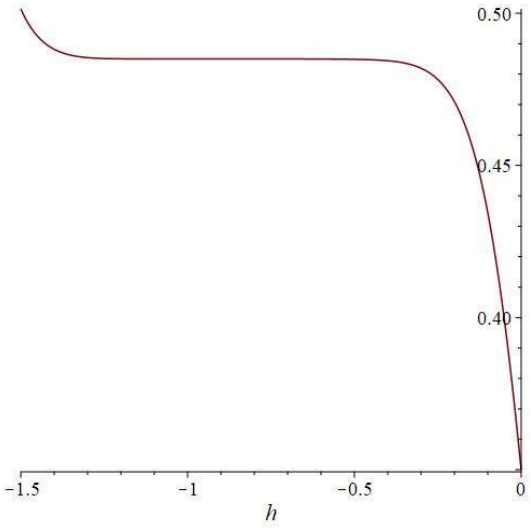

Figure 13. The h-curve representation of ninth-order HAMFF lower solution for system (24) of $\underline{v}(0.1; 0.5; h)$.

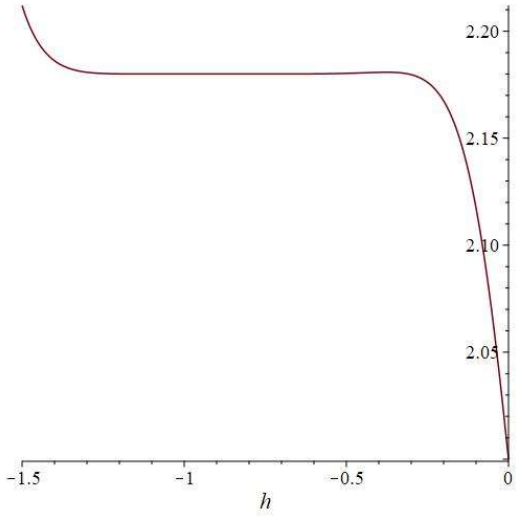

Figure 14. The h-curve representation of ninth-order HAMFF upper solution for system (24) of $\overline{v}(0.1; 0.5; h)$.

Table 10. Best values of the convergence control parameter of ninth-order fuzzy HAMFF solution $\tilde{u}(x, \alpha)$ of system (24) at $x = 0.1$ and $\alpha = 0.5$, where * denoted to the optimal value of $\tilde{h}_1$.

$\underline{\boldsymbol{h}}_{\boldsymbol{11}}$*	-0.994760367994695203
$\overline{\boldsymbol{h}}_{\boldsymbol{11}}$*	-0.991888973708002525

Table 11. Best values of the convergence control parameter of ninth-order HAMFF solution $\tilde{v}(x, \alpha)$ of system (24) at $x = 0.1$ and $\alpha = 0.5$, where * denoted to the optimal value of $\tilde{h}_2$.

$\underline{\boldsymbol{h}}_{\boldsymbol{21}}$*	-0.994874792763616010
$\overline{\boldsymbol{h}}_{\boldsymbol{21}}$*	-0.985659503042079665

By comparing the Tables 12–15, we can see how the results improve after the minimization process.

Table 12. Solution and accuracy of ninth-order HAMFF for system (24) of $\tilde{u}(x, \alpha)$ at $x = 0.5$ and $\tilde{h}_i = -1$ with $0 \leq \alpha \leq 1$.

α	$\underline{u}_E(x, \alpha)$	$\underline{u}(x, \alpha)$	$\lvert\underline{u}_E(x, \alpha) - \underline{u}(x, \alpha)\rvert$	$\overline{u}_E(x, \alpha)$	$\overline{u}(x, \alpha)$	$\lvert\overline{u}_E(x, \alpha) - \overline{u}(x, \alpha)\rvert$
0.0	1.000	1.000000001	1.382E-09	3.500	3.500000005	5.577E-09
0.2	1.250	1.250000001	1.801E-09	3.250	3.250000005	5.157E-09
0.4	1.500	1.500000002	2.221E-09	3.000	3.000000004	4.738E-09
0.6	1.750	1.750000002	2.640E-09	2.750	2.750000004	4.318E-09
0.8	2.000	2.000000003	3.060E-09	2.500	2.500000003	3.899E-09
1.0	2.250	2.250000003	3.479E-09	2.250	2.250000003	3.479E-09

Table 13. Solution and accuracy ninth-order HAMFF for system (24) of $\tilde{v}(x,\alpha)$ at $x = 0.5$ and $\tilde{h}_i = -1$ with $0 \le \alpha \le 1$.

α	$\underline{v}_E(x,\alpha)$	$\underline{v}(x,\alpha)$	$\lvert\underline{v}_E(x,\alpha) - \underline{v}(x,\alpha)\rvert$	$\overline{v}_E(x,\alpha)$	$\overline{v}(x,\alpha)$	$\lvert\overline{v}_E(x,\alpha) - \overline{v}(x,\alpha)\rvert$
0.0	-1.000	-1.000000004	4.770E-09	3.500	3.499999996	3.408E-09
0.2	-0.550	-0.550000004	4.634E-09	3.050	3.049999996	3.544E-09
0.4	-0.100	-0.100000004	4.498E-09	2.600	2.599999996	3.681E-09
0.6	0.350	0.349999995	4.362E-09	2.150	2.149999996	3.817E-09
0.8	0.800	0.799999995	4.225E-09	1.700	1.699999996	3.953E-09
1.0	1.250	1.249999995	4.089E-09	1.250	1.249999995	4.089E-09

Tables 12 and 13 show a comparison of the absolute errors applying the HAMFF $(m = 9)$ with the exact solutions within the interval $0 \le \alpha \le 1$ at $x = 0.5$ with best values of the convergence control parameter $\tilde{h}_i$ after minimization which are listed in the following tables (see Tables 14 and 15).
The values of $\tilde{C}_1$, and $\tilde{C}_2$, at $x = 1$ for $0 \le \alpha \le 1$ with optimal values of $\tilde{h}_i$ calculated from the BCs (25) are as follows

$$\underline{C}_1 = -2.2133 \times 10^{-9} - 1.999999995\alpha, \quad \overline{C}_1 = -3.999999995 + 1.999999995\alpha,$$
$$\underline{C}_2 = -1.000000005 + 2.000000005\alpha, \quad \overline{C}_2 = 3.000000023 - 2.000000015\,\alpha.$$

Table 14. Solution and accuracy ninth-order HAMFF for system (24) of $\tilde{u}(x,\alpha)$ at $x = 0.1$ and $\tilde{h}_i = \underline{h}_{11}$, $\tilde{h}_i = \overline{h}_{11}$with $0 \le \alpha \le 1$.

α	$\underline{u}_E(x,\alpha)$	$\underline{u}(x,\alpha)$	$\lvert\underline{u}_E(x,\alpha) - \underline{u}(x,\alpha)\rvert$	$\overline{u}_E(x,\alpha)$	$\overline{u}(x,\alpha)$	$\lvert\overline{u}_E(x,\alpha) - \overline{u}(x,\alpha)\rvert$
0.0	1.0	0.999999998	1.112E-09	3.50	3.500000002	2.503E-09
0.2	1.250	1.249999999	6.640E-10	3.250	3.250000002	2.042E-09
0.4	1.500	1.499999999	2.154E-10	3.000	3.000000001	1.581E-09
0.6	1.750	1.750000000	2.331E-10	2.750	2.750000001	1.120E-09
0.8	2.000	2.000000000	6.817E-10	2.500	2.500000000	6.599E-10
1.0	2.250	2.250000001	1.130E-09	2.250	2.250000000	1.990E-10

Table 15. Solution and accuracy ninth-order HAMFF for system (24) of $\tilde{v}(x,\alpha)$ at $x = 0.1$ and $\tilde{h}_i = \underline{h}_{21}$, $\tilde{h}_i = \overline{h}_{21}$with $0 \le \alpha \le 1$.

α	$\underline{v}_E(x,\alpha)$	$\underline{v}(x,\alpha)$	$\lvert\underline{v}_E(x,\alpha) - \underline{v}(x,\alpha)\rvert$	$\overline{v}_E(x,\alpha)$	$\overline{v}(x,\alpha)$	$\lvert\overline{v}_E(x,\alpha) - \overline{v}(x,\alpha)\rvert$
0.0	-1.000	-1.000000002	2.752E-09	3.500	3.500000011	1.140E-08
0.2	-0.550	-0.550000002	2.194E-09	3.050	3.050000009	9.896E-09
0.4	-0.100	-0.100000001	1.636E-09	2.600	2.600000008	8.389E-09
0.6	0.350	0.349999998	1.078E-09	2.150	2.150000006	6.882E-09
0.8	0.800	0.799999999	5.201E-10	1.700	1.700000005	5.375E-09
1.0	1.250	1.250000000	3.791E-11	1.250	1.250000003	3.868E-09

In the following Figures 15–20 shows that the exact solutions ($\tilde{u}_E(x,\alpha)$, $\tilde{v}_E(x,\alpha)$) and the fuzzy approximate solutions by HAMFF ($\tilde{u}(x,\alpha)$, $\tilde{v}(x,\alpha)$) of the system (24) are in the form of fuzzy numbers for any $0 \le \alpha \le 1$ at $x = 0.1$ and $\tilde{h}_i = -1$.

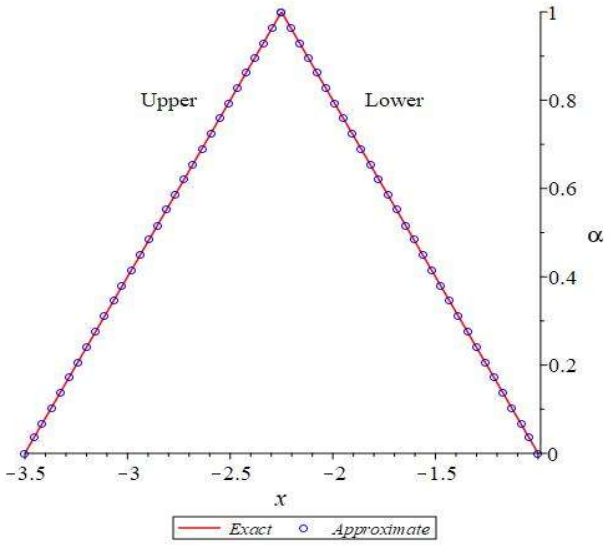

Figure 15. The exact and HAMFF lower and upper solutions of system (24) $\tilde{u}_E(x,\alpha)$ and $\tilde{u}(x,\alpha)$ for all $\alpha \in [0,1]$.

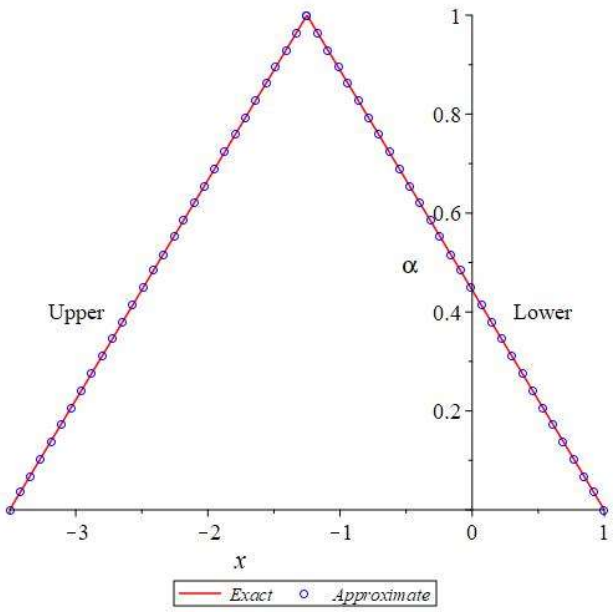

Figure 16. The exact and HAMFF lower and upper solutions of system (24) $\tilde{v}_E(x,\alpha)$ and $\tilde{v}(x,\alpha)$ for all $\alpha \in [0,1]$.

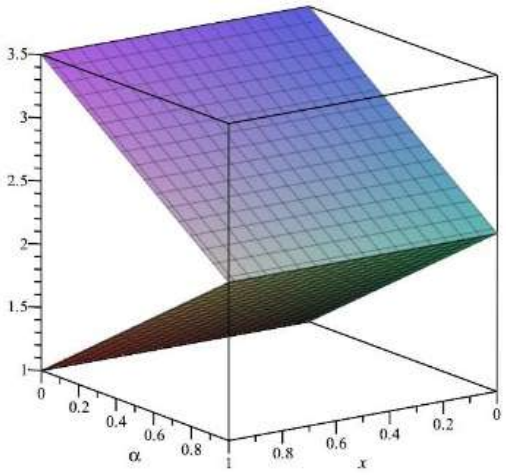

Figure 17. The exact lower and upper solutions of system (24) $\tilde{u}_E(x,\alpha)$ for all $x,\alpha \in [0,1]$.

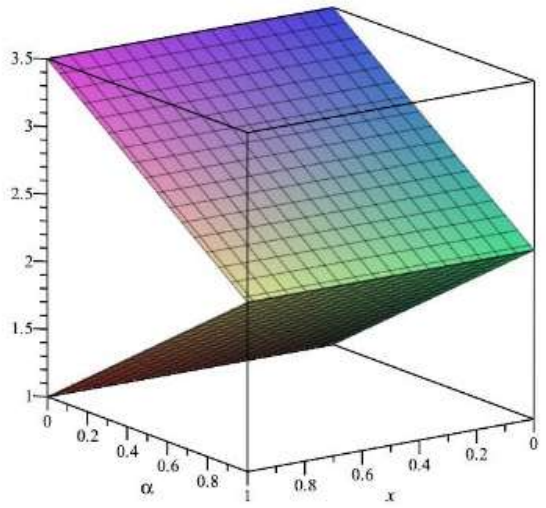

Figure 18. The HAMFF lower and upper solutions of system (24) and $\tilde{u}(x,\alpha)$ for all $x,\alpha \in [0,1]$.

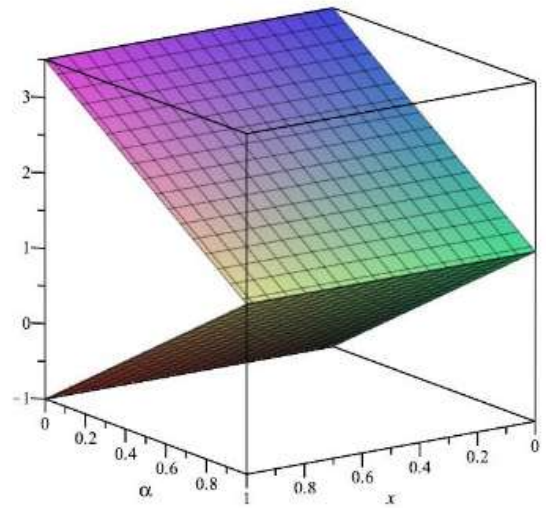

Figure 19. The exact lower and upper solutions of system (24) $\tilde{v}_E(x,\alpha)$ for all $x,\alpha \in [0,1]$.

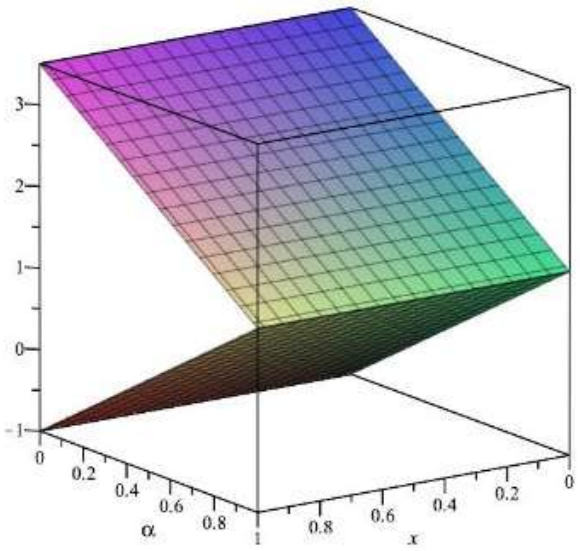

Figure 20. The HAMFF lower and upper solutions of system (24) and $\tilde{v}(x,\alpha)$ for all $x,\alpha \in [0,1]$.

According to Figures 15–20, one can summarize that the ninth-order HAMFF solutions of system (24) satisfied the fuzzy solution in triangular fuzzy number forms are illustrated in Tables 16 and 17. Next, a comparison between ninth-order HAMFF solution and the MLP [11] are displayed in Table 18 in terms of accuracy at different values of $x \in [0,1]$ and $\alpha = 1$.

The values of C_1, and C_2, at $x = 1$ for $\alpha = 1$ calculated from the BCs (22) are as follows

$$C_1 = -1.999999993, \quad C_2 = 0.999999991.$$

Table 16. Accuracy of ninth-order HAMFF solution for system (24) at $\alpha = 1$ and $h_i = -1$.

x	$u_E(x,1)$	$u(x,1)$	$\lvert u_E(x,1) - u(x,1)\rvert$	$v_E(x,1)$	$v(x,1)$	$\lvert v_E(x,1) - v(x,1)\rvert$
0.0	3.0	3.0	0.0	1.0	1.0	0.0
0.2	2.64	2.640000001	1.357E-09	1.16	1.159999998	1.652E-09
0.4	2.36	2.360000002	2.732E-09	1.24	1.239999996	3.240E-09
0.6	2.16	2.160000004	4.374E-09	1.24	1.239999994	5.138E-09
0.8	2.04	2.040000006	6.953E-09	1.16	1.159999991	8.385E-09
1.0	2.00	1.999999999	0.0	1.00	0.999999999	0.0

Table 17. Control parameters at $\alpha = 1$, where h_i is the ideal expression.

h_{11}*	-0.989174220493120112
h_{21}*	-0.988661974289768555

The values of C_1, and C_2, at $x = 1$ for $\alpha = 1$ with optimal values of $h_i$calculated from the BCs (22) as follows

$$C_1 = -2.000000000, \quad C_2 = 1.000000006.$$

Table 18. Accuracy of ninth-order HAMFF solution and MLP [11] for system (24) at $\alpha = 1$ and h_i with optimal values of $h_1 = \underline{h}_{11}$, $h_2 = \overline{h}_{21}$.

x	$u_E(x,1)$	$u(x,1)$	$\lvert u_E(x,1) - u(x,1)\rvert$	$v_E(x,1)$	$v(x,1)$	$\lvert v_E(x,1) - v(x,1)\rvert$
0.0	3.0	3.0	0.0	1.0	1.0	0.0
0.2	2.64	2.639999999	1.799E-10	1.16	1.160000001	1.300E-09
0.4	2.36	2.359999999	2.774E-10	1.24	1.240000002	2.510E-09
0.6	2.16	2.159999999	1.135E-10	1.24	1.240000003	3.377E-09
0.8	2.04	2.040000001	1.026E-09	1.16	1.160000002	2.664E-09
1.0	2.00	2.000000000	0.0	1.00	0.999999999	0.0

From Table 18, the ninth-order HAMFF solution system (9) obtained better solution in terms of accuracy MLP [11] at
$\alpha = 1$ at different values of x .

Problem 3. From [4] the fuzzy version of second kind linear SFIDEs is defined as below:

$$\begin{aligned} \tilde{u}'(x,\alpha) &= \tilde{f}_1(x,\alpha) + \int_0^1 \left[\frac{xt}{2}\tilde{u}(t,\alpha) - x\tilde{v}(t,\alpha)\right] dt\,, \\ \tilde{v}'(x,\alpha) &= \tilde{f}_2(x,\alpha) + \int_0^1 \left[x^2\tilde{u}(t,\alpha) - \frac{x^2 t}{2}\tilde{v}(t,\alpha)\right] dt\,, \end{aligned} \tag{35}$$

with the ICs

$$\tilde{u}(0,\alpha) = (\alpha - 1, 1 - \alpha), \ \tilde{v}(0,\alpha) = (1 - \alpha, \alpha - 1), \tag{36}$$

where

$$\tilde{f}_1(x,\alpha) = \left[\underline{f_1}(x,\alpha), \overline{f}_1(x,\alpha)\right] = \left[\frac{7}{16}\alpha x, \left(\frac{9}{8} - \frac{11}{16}\alpha\right)x\right],$$

and

$$\tilde{f}_2(x,\alpha) = \left[\underline{f_2}(x,\alpha), \overline{f}_2(x,\alpha)\right] = \left[\frac{169}{30}\alpha x^2, \left(\frac{251}{30} - \frac{164}{60}\alpha\right)x^2\right].$$

Section 3 of the HAMFF analysis of system (35) states the following:

$$\begin{aligned} \tilde{u}_0(x,\alpha) &= \tilde{u}(0,\alpha), \\ \tilde{v}_0(x,\alpha) &= \tilde{v}(0,\alpha), \end{aligned} \tag{37}$$

and choosing the linear operators

$$\begin{aligned} L[\tilde{u}(x,q,\alpha)] &= \frac{\partial \tilde{u}(x,q,\alpha)}{\partial x}, \\ L[\tilde{v}(x,q,\alpha)] &= \frac{\partial \tilde{v}(x,q,\alpha)}{\partial x}, \end{aligned} \quad L^{-1} = \int_0^x (\cdot)dt,$$

with the property $L[c_1] = 0$, where c_1 is a constant. Furthermore, the system (35) suggests that we define the nonlinear operators as

$$\begin{cases} N_1[\tilde{u}(x,q,\alpha),\tilde{v}(x,q,\alpha)] = \frac{\partial \tilde{u}(x,q,\alpha)}{\partial x} - \tilde{f}_1(x,\alpha) \\ \quad - \int_0^1 \left[\frac{xt}{2}\tilde{u}(x,q,\alpha) + x\tilde{v}(x,q,\alpha)\right] dt\,, \\ N_2[\tilde{u}(x,q,\alpha),\tilde{v}(x,q,\alpha)] = \frac{\partial \tilde{v}(x,q,\alpha)}{\partial x} - \tilde{f}_2(x,\alpha) \\ \quad - \int_0^1 \left[x^2\tilde{v}(x,q,\alpha) + \frac{x^2 t}{2}\tilde{u}(x,q,\alpha)\right] dt\,. \end{cases} \tag{38}$$

Using the above definition, with the assumption $H(x) = 1$, we construct the zeroth-order deformation equation

$$\begin{cases} (1-q)L[\tilde{u}(x,q,\alpha) - \tilde{u}_0(x,\alpha)] = qhH(x)N_1[\tilde{u}(x,q,\alpha),\tilde{v}(x,q,\alpha)], \\ (1-q)L[\tilde{v}(x,q,\alpha) - \tilde{v}_0(x,\alpha)] = qhH(x)N_2[\tilde{u}(x,q,\alpha),\tilde{v}(x,q,\alpha)]. \end{cases} \tag{39}$$

Obviously, when $q = 0$ and $q = 1$
$\tilde{u}(x,0,\alpha) = \tilde{u}_0(x,\alpha), \quad \tilde{u}(x,1,\alpha) = \tilde{u}(x,\alpha),$
$\tilde{v}(x,0,\alpha) = \tilde{v}_0(x,\alpha), \quad \tilde{v}(x,1,\alpha) = \tilde{v}(x,\alpha),$
Thus, we obtain the $mth-$order deformation equations for $m \geq 1$ which are

$$\begin{cases} L[\tilde{u}_m(x,\alpha) - \chi_m \tilde{u}_{m-1}(x,\alpha)] = h\left[R_{1,m}\left(\vec{\tilde{u}}_{m-1}, \vec{\tilde{v}}_{m-1}\right)\right], \\ L[\tilde{v}_m(x,\alpha) - \chi_m \tilde{v}_{m-1}(x,\alpha)] = h\left[R_{2,m}\left(\vec{\tilde{u}}_{m-1}, \vec{\tilde{v}}_{m-1}\right)\right], \end{cases} \tag{40}$$

where

$$\begin{aligned} R_{1,m}\left(\vec{\tilde{u}}_{m-1}, \vec{\tilde{v}}_{m-1}\right) &= \tilde{u}'_{m-1}(x,\alpha) - (1-\chi_m)\tilde{f}_1(x,\alpha) \\ &\quad - \int_0^1 \left[\frac{xt}{2}\tilde{u}_{m-1}(t,\alpha) + x\tilde{v}_{m-1}(t,\alpha)\right] dt\,, \\ R_{2,m}\left(\vec{\tilde{u}}_{m-1}, \vec{\tilde{v}}_{m-1}\right) &= \tilde{v}'_{m-1}(x,\alpha) - (1-\chi_m)\tilde{f}_2(x,\alpha) \\ &\quad - \int_0^1 \left[x^2\tilde{u}_{m-1}(t,\alpha) + \frac{x^2 t}{2}\tilde{v}_{m-1}(t,\alpha)\right] dt\,. \end{aligned} \tag{41}$$

Now, for $m \geq 1$, the solutions of the *mth*-order deformation system (35) are

$$\begin{cases} \tilde{u}_m(x,\alpha) = \chi_m \tilde{u}_{m-1}(x,\alpha) + hL^{-1}\left[R_{1,m}\left(\vec{\tilde{u}}_{m-1}, \vec{\tilde{v}}_{m-1}\right)\right], \\ \tilde{v}_m(x,\alpha) = \chi_m \tilde{v}_{m-1}(x,\alpha) + hL^{-1}\left[R_{2,m}\left(\vec{\tilde{u}}_{m-1}, \vec{\tilde{v}}_{m-1}\right)\right]. \end{cases} \tag{42}$$

Thus, the approximate solutions in a series form are given by

$$\begin{aligned} \tilde{u}(x,\alpha) &= \tilde{u}_0(x,\alpha) + \textstyle\sum_{k=1}^{9} \tilde{u}_k(x,\alpha)\,, \\ \tilde{v}(x,\alpha) &= \tilde{v}_0(x,\alpha) + \textstyle\sum_{k=1}^{9} \tilde{v}_k(x,\alpha)\,. \end{aligned} \tag{43}$$

The residual error function with respect to this solution for the system (32) is

$$\begin{aligned} \widetilde{RE}_1(x,\alpha) &= \tilde{u}'(x,\alpha) - \tilde{f}_1(x,\alpha) - \int_0^1 \left[\frac{xt}{2}\tilde{u}(t,\alpha) + x\tilde{v}(t,\alpha)\right] dt\,, \\ \widetilde{RE}_2(x,\alpha) &= \tilde{v}'(x,\alpha) - \tilde{f}_2(x,\alpha) - \int_0^1 \left[x^2\tilde{u}(t,\alpha) + \frac{x^2 t}{2}\tilde{v}(t,\alpha)\right] dt\,. \end{aligned} \tag{44}$$

The $\tilde{h}_i(\alpha)$-curves of ninth-order HAMFF upper and lower bound solutions $\tilde{u}(x,\alpha)$ and $\tilde{v}(x,\alpha)$ at $x = 0.5$ and $\alpha = 0.5$ for system (35) are shown in the following Tables 19 and 20 and Figures 21–24.

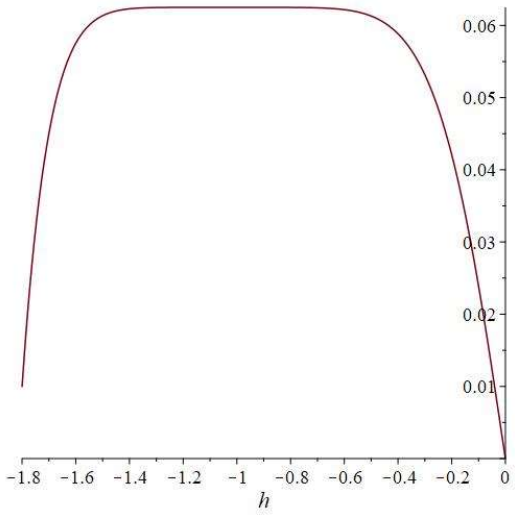

Figure 21. The h-curve representation of ninth-order HAMFF lower solution for system (35) of $\underline{u}(0.5; 0.5; h)$.

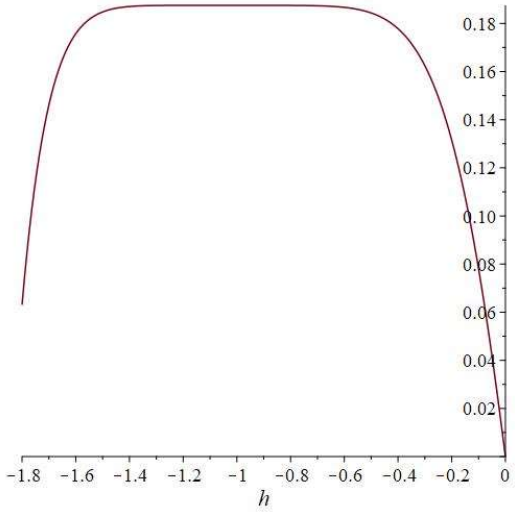

Figure 22. The h-curve representation of ninth-order HAMFF upper solution for system (35) of $\overline{u}(0.5; 0.5; h)$.

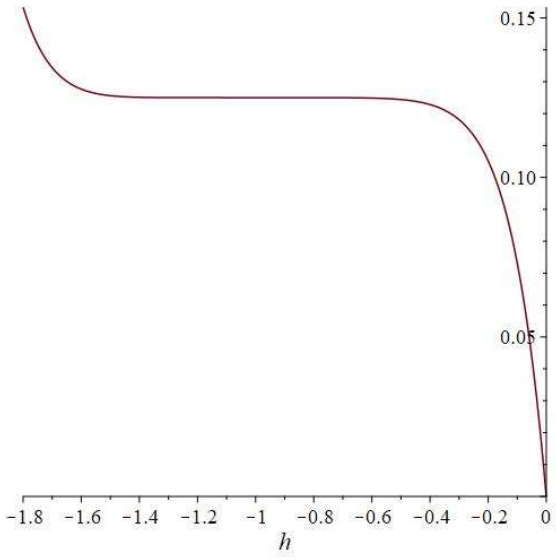

Figure 23. The h-curve representation of ninth-order HAMFF lower solution for system (35) of $\underline{v}(0.5; 0.5; h)$.

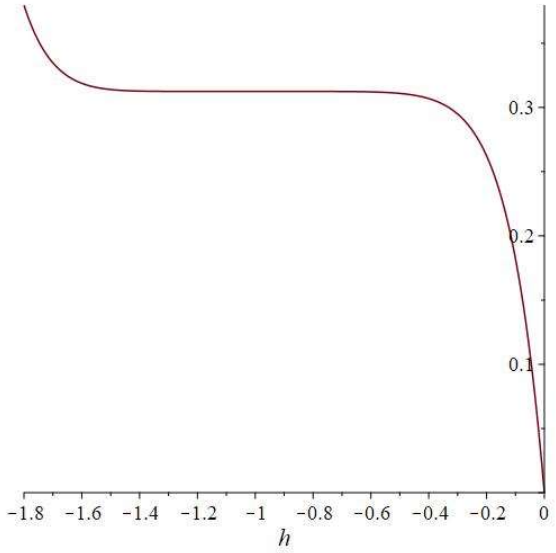

Figure 24. The h-curve representation of ninth-order HAMFF upper solution for system (35) of $\overline{v}(0.5; 0.5; h)$.

Table 19. Best values of the convergence control parameter of ninth-order HAMFF solution $\tilde{u}(x, \alpha)$ of system (35) at $x = 0.5$ and $\alpha = 0.5$, where * denoted to the optimal value of $\tilde{h}_1$.

$\underline{\boldsymbol{h}}_{\mathbf{11}}$*	-1.050070264612211042266285916 48
$\overline{\boldsymbol{h}}_{\mathbf{11}}$*	-1.050900020609144722448686357 90

Table 20. Best values of the convergence control parameter of ninth-order HAMFF solution $\tilde{v}(x,\alpha)$ of system (35) at $x = 0.5$ and $\alpha = 0.5$, where * denoted to the optimal value of $\tilde{h}_2$.

$\underline{\boldsymbol{h}}_{\boldsymbol{21}}$*	-1.050127283391936041333712090 84
$\overline{\boldsymbol{h}}_{\boldsymbol{21}}$*	-1.050862851440531362043304400 90

In order to validate the ninth-order HAMFF solution of system (32), a comparative analysis with the learning algorithm iteration (LAI) [4] corresponding with 200 iteration is displayed in Tables 21 and 22 in terms of residual errors $(\widetilde{RE}_1)$ and $(\widetilde{RE}_2)$ respectively for different values of $0 \le \alpha \le 1$ at $x = 0.5$.

By comparing the Tables 21–23, we can see how the results improve after the minimization process. A comparison between ninth-order HAM solution and the fuzzy neural network [4] with 200 numerical iterations is given.

Table 21. Show a comparison of the REs $(\widetilde{RE}_1)$ applying the HAMFF $(m = 9)$ and LAI [4] within the interval $0 \le \alpha \le 1$ at $x = 0.5$ and $\tilde{h}_i = -1$.

α	$\underline{u}(x,\alpha)$	$\underline{RE}_1(x,\alpha)$	LAI [4]	$\overline{u}(x,\alpha)$	$\overline{RE}_1(x,\alpha)$	LAI [4]
0.0	0.0	0.0	0.0	0.249999946	1.770E-07	8.72E-06
0.2	0.024999993	2.205E-08	1.30E-07	0.224999950	1.636E-07	6.50E-07
0.4	0.049999986	4.411E-08	3.30E-07	0.199999954	1.503E-07	6.30E-07
0.6	0.074999980	6.617E-08	2.60E-07	0.174999958	1.369E-07	4.50E-07
0.8	0.099999973	8.823E-08	1.40E-07	0.149999962	1.236E-07	4,70E-07
1.0	0.124999966	1.102E-07	1.40E-07	0.124999966	1.102E-07	1.40E-07

Table 22. Show a comparison of the REs $(\widetilde{RE}_2)$ applying the HAMFF $(m = 9)$ and LAI [4] within the interval $0 \le \alpha \le 1$ at $x = 0.5$ and $\tilde{h}_i = -1$.

α	$\underline{v}(x,\alpha)$	$\underline{RE}_2(x,\alpha)$	LAI [4]	$\overline{v}(x,\alpha)$	$\overline{RE}_2(x,\alpha)$	LAI [4]
0.0	0.0	0.0	0.0	0.374999977	1.105E-07	3.01E-06
0.2	0.049999997	1.377E-08	3.50E-07	0.349999979	1.022E-07	2.20E-06
0.4	0.099999994	2.755E-08	4.40E-07	0.324999981	9.389E-08	2.13E-06
0.6	0.149999991	4.132E-08	6.60E-07	0.299999982	8.555E-08	2.10E-06
0.8	0.199999988	5.510E-08	2.40E-07	0.274999984	7.721E-08	1.32E-06
1.0	0.249999986	6.887E-08	1.12E-06	0.249999986	6.887E-08	1.24E-06

Tables 21 and 22 show a comparison of the REs applying the HAMFF $(m = 9)$ with the errors [4] within the interval $0 \le \alpha \le 1$ at $x = 0.5$ with best values of the convergence control parameter $\tilde{h}_i$ after minimization which are listed in the following tables (see Table 23).

Table 23. REs applying the HAMFF $(m = 9)$ at $x = 0.5$ and $\tilde{h}_i$ are optimal values of $\tilde{h}_{ij}$.

α	$\underline{u}(x,\alpha)$	$\underline{RE}_1(x,\alpha)$	$\overline{u}(x,\alpha)$	$\overline{RE}_1(x,\alpha)$	$\underline{v}(x,\alpha)$	$\underline{RE}_2(x,\alpha)$	$\overline{v}(x,\alpha)$	$\overline{RE}_2(x,\alpha)$
0.0	0.0	0.0	0.249999994	2.190E-08	0.0	0.0	0.374999999	4.495E-10
0.2	0.024999999	2.928E-09	0.224999994	2.045E-08	0.049999999	1.234E-13	0.349999999	2.552E-10
0.4	0.049999998	5.856E-09	0.199999994	1.900E-08	0.099999999	2.468E-13	0.324999999	6.091E-11
0.6	0.074999997	8.784E-09	0.174999995	1.755E-08	0.149999999	3.703E-13	0.299999999	1.333E-10
0.8	0.099999996	1.171E-08	0.149999995	1.610E-08	0.199999999	4.937E-13	0.274999999	3.276E-10
1.0	0.124999996	1.464E-08	0.124999996	1.464E-08	0.249999999	6.171E-13	0.249999999	5.220E-10

In the following Figures 25–28 show that the fuzzy approximate solutions by HAMFF $(\tilde{u}(x,\alpha),\ \tilde{v}(x,\alpha))$ of the system (32) are in the form of fuzzy numbers for any $0 \leq \alpha \leq 1$ at $x = 0.5$ and $\tilde{h}_i = -1$.

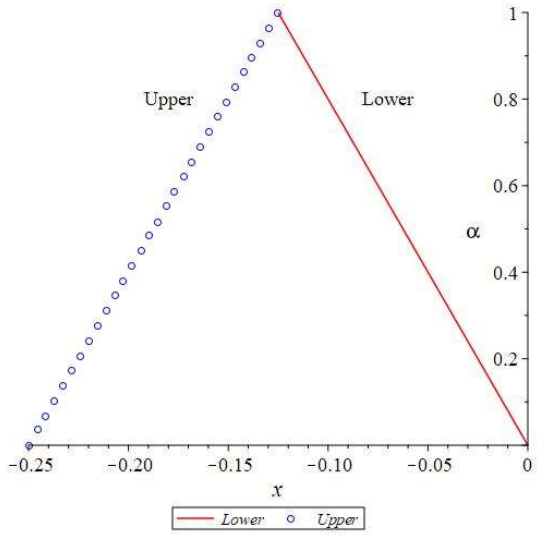

Figure 25. The HAM lower and upper solutions of system (35) $\tilde{u}(x,\alpha)$ for all $\alpha \in [0,1]$.

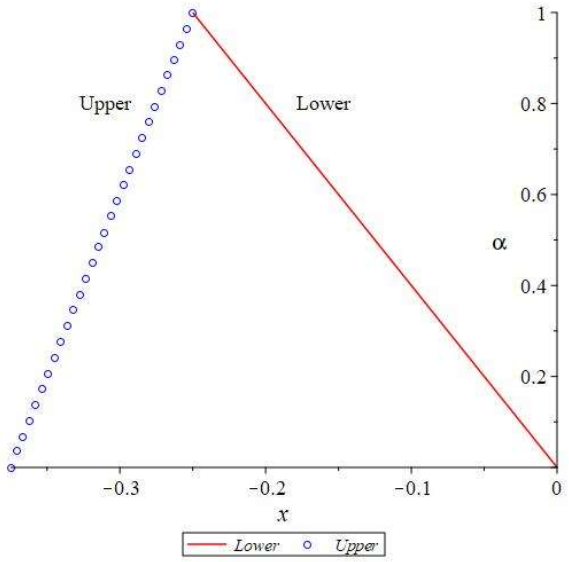

Figure 26. The HAM lower and upper solutions of system (35) $\tilde{v}(x,\alpha)$ for all $\alpha \in [0,1]$.

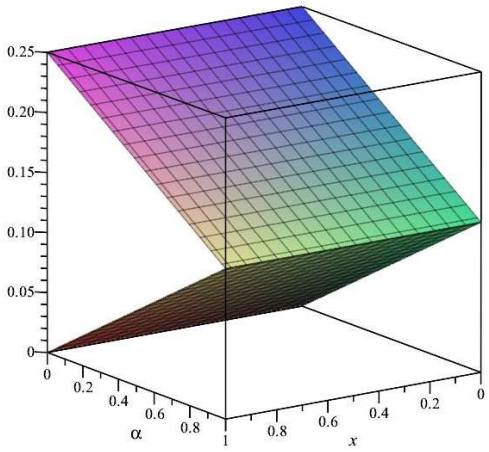

Figure 27. The HAMFF lower and upper solutions of system (35) and $\tilde{u}(x,\alpha)$ for all $x,\alpha \in [0,1]$.

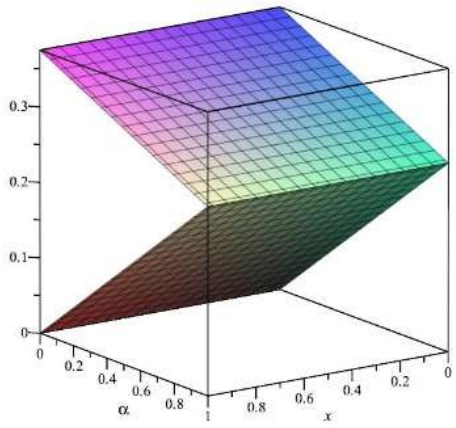

Figure 28. The HAMFF lower and upper solutions of system (35) and $\tilde{v}(x,\alpha)$ for all $x,\alpha \in [0,1]$.

The fuzzy solution in triangular fuzzy number forms was satisfied by the ninth-order HAMFF solutions of system (35) as shown in Figures 25–28.

6. Conclusions

The method of approximate analytical class for solving FSIDEs, known as HAMFF, is the main topic of this work. Using the HAMFF technique, the convergence of the series solution can be efficiently managed by selecting the best convergence parameter for each fuzzy level set. In this study, the FSFIDEs were proposed as utilized as an experimental study to demonstrate the HAMFF technique's precision in solving linear systems with initial conditions. The technique was found to produce a polynomial series solution in close-analytical form that converges to the exact solution as the series order increases. The novelty of HAMFF derived from basic concepts of the standard HAM and some popular definitions and properties of fuzzy sets theory. The study also used the HAMFF to find the series solution in nonlinear terms and suggested a new fuzzy version of FSFIDEs. The HAMFF technique was discovered to offer the series solution FSFIDEs subject to boundary conditions. The optimal convergence parameters for the suggested problems were also ascertained by utilizing the HAMFF's convergence behavior in fuzzy environments to increase the accuracy of the technique. A comparison analysis between the HAMFF and other approximate techniques is presented, showing that the HAMFF obtained a better solution in terms of accuracy. It is noteworthy to note that all the problems in this study that were solved with HAMFF obtained the series solution in the triangular fuzzy numbers.

Author contributions

Zena Talal Yassin: Conceptualization, validation, investigation, writing original draft preparation; Waleed Al-Hayani: Conceptualization, validation, investigation, writing original draft preparation; Ala Amourah: methodology, validation, writing review and editing; Ali F. Jameel: methodology, for-mal analysis, writing review and editing; Nidal Anakira: methodology, investigation, supervision; All authors have read and agreed to the published version of the manuscript.

Use of Generative-AI tools declaration

The authors declare they have not used Artificial Intelligence (AI) tools in the creation of this article.

Conflict of interest

The authors declare no conflict of interest.

References

1. J. Chen, M. He, T. Zeng, A multiscale Galerkin method for second-order boundary value problems of Fredholm integro-differential equation II: Efficient algorithm for the discrete linear system, *J. Vis. Commun. Image R.*, **58** (2019), 112–118. https://doi.org/10.1016/j.jvcir.2018.11.027
2. G. G. Biçer, Y. Öztürk, M. Gülsu, Numerical approach for solving linear Fredholm integro-differential equation with piecewise intervals by Bernoulli polynomials, *Int. J. Comput. Math.*, **95** (2018), 2100–2111. https://doi.org/10.1080/00207160.2017.1366458
3. A. Jameel, N. R. Anakira, A. K. Alomari, I. Hashim, M. A. Shakhatreh, Numerical solution of n'th order fuzzy initial value problems by six stages, *J. Nonlinear Sci. Appl.*, **9** (2016), 627–640. https://doi.org/10.22436/jnsa.009.02.26
4. M. Mosleh, M. Otadi, Simulation and evaluation of system of fuzzy linear Fredholm integro-differential equations with fuzzy neural network, *Neural Comput. Appl.*, **31** (2019), 3481–3491. https://doi.org/10.1007/s00521-017-3267-2
5. N. R. Anakira, A. K. Alomari, A. F. Jameel, I. Hashim, Multistage optimal homotopy asymptotic method for solving initial-value problems, *J. Nonlinear Sci. Appl.,* **9** (2016), 1826–1843. https://doi.org/10.22436/jnsa.009.04.37
6. L. Zada, M. Al-Hamami, R. Nawaz, S. Jehanzeb, A. Morsy, A. Abdel-Aty, et al., A new approach for solving Fredholm integro-differential equations, *Inf. Sci. Lett.*, **10** (2021), 407–415. https://doi.org/10.18576/isl/100303
7. M. El-Gamel, O. Mohamed, Nonlinear second order systems of Fredholm integro-differential equations, *SeMA J.*, **79** (2022), 383–396. https://doi.org/10.1007/s40324-021-00258-x
8. Ş. Yüzbaşı, N. Şahin, M. Sezer, Numerical solutions of systems of linear Fredholm integro-differential equations with Bessel polynomial bases, *Comput. Math. Appl.*, **61** (2011), 3079–3096. https://doi.org/10.1016/j.camwa.2011.03.097

9. F. Mirzaee, S. F. Hoseini, Solving systems of linear Fredholm integro-differential equations with Fibonacci polynomials, *Ain Shams Eng. J.*, **5** (2014), 271–283. https://doi.org/10.1016/j.asej.2013.09.002
10. F. Mirzaee, S. Bimesl, Numerical solutions of systems of high-order Fredholm integro-differential equations using Euler polynomials, *Appl. Math. Model.*, **39** (2015), 6767–6779. https://doi.org/10.1016/j.apm.2015.02.022
11. Z. Elahi, G. Akram, S. S. Siddiqi, Laguerre approach for solving system of linear Fredholm integro-differential equations, *Math. Sci.*, **12** (2018), 185–195. https://doi.org/10.1007/s40096-018-0258-0
12. M. Ghasemi, K. Mohammadi, A. Alipanah, Numerical solution of system of second-order integro-differential equations using nonclassical sinc collocation method, *Bound. Value Probl.*, **2023** (2023), 38. https://doi.org/10.1186/s13661-023-01724-3
13. D. Dubois, H. Prade, Towards fuzzy differential calculus part 3: Differentiation, *Fuzzy Set. Syst.*, **8** (1982), 225–233. https://doi.org/10.1016/S0165-0114(82)80001-8
14. M. Friedman, M. Ma, A. Kandel, Numerical solutions of fuzzy differential and integral equations, *Fuzzy Set. Syst.*, **106** (1999), 35–48. https://doi.org/10.1016/S0165-0114(98)00355-8
15. S. Hasan, A. Alawneh, M. Al-Momani, S. Momani, Second order fuzzy fractional differential equations under Caputo's H-differentiability, *Appl. Math. Inf. Sci*, **11** (2017), 1597–1608. https://doi.org/10.18576/amis/110606
16. S. M. Far, M. A. Firozja, A. A. Hosseinzadeh, B. Agheli, An approximate solution of Riccati's differential equation using fuzzy linguistic model, *Soft Comput.*, **25** (2021), 8627–8633. https://doi.org/10.1007/s00500-021-05789-z
17. A. Georgieva, Solving two-dimensional nonlinear fuzzy Volterra integral equations by homotopy analysis method, *Demonstr. Math.*, **54** (2021), 11–24. https://doi.org/10.1515/dema-2021-0005
18. S. J. Liao, *The proposed homotopy analysis technique for the solution of nonlinear problems,* (Doctoral dissertation, Ph. D. Thesis, Shanghai Jiao Tong University), 1992.
19. N. Anakira, O. Oqilat, A. Almalki, I. Irianto, S. Meqdad, A. Amourah, Numerical proceduers for computing the exact solutions to systems of ordinary differential equations, *Int. J. Neutrosophic Sci.*, **2** (2025), 165–65.
20. S. A. Altaie, N. Anakira, A. Jameel, O. Ababneh, A. Qazza, A. K. Alomari, Homotopy analysis method analytical scheme for developing a solution to partial differential equations in fuzzy environment, *Fractal Fract.*, **6** (2022), 419. https://doi.org/10.3390/fractalfract6080419
21. N. Anakira, A. Almalki, M. J. Mohammed, S. Hamad, O. Oqilat, A. Amourah, et al., Analytical approaches for computing exact solutions to system of Volterra integro-differential equations, *WSEAS T. Math.,* **23** (2024), 400–407. https://doi.org/10.37394/23206.2024.23.43
22. D. J. Hashim, A. F. Jameel, T. Y. Ying, Approximate solutions of fuzzy fractional differential equations via homotopy analysis method, *Prog. Fract. Differ. Appl.*, **9** (2023), 167–187. https://doi.org/10.18576/pfda/090112
23. E. A. Hussain, A. W. Ali, Homotopy analysis method for solving fuzzy integro-differential equations, *Mod. Appl. Sci.*, **7** (2013), 15. https://doi.org/10.5539/mas.v7n3p15
24. S. Bodjanova, Median alpha-levels of a fuzzy number, *Fuzzy Set. Syst.*, **157** (2006), 879–891. https://doi.org/10.1016/j.fss.2005.10.015

25. A. F. Jameel, N. Anakira, A. K. Alomari, I. Hashim, S. Momani, A new approximation method for solving fuzzy heat equations, *J. Comput. Theor. Nanos.*, **13** (2016), 7825–7832. https://doi.org/10.1166/jctn.2016.5784
26. G. J. Klir, B. Yuan, *Fuzzy sets and fuzzy logic: Theory and applications*, New Jersey: Prentice Hall, **4** (1995), 1–12.
27. O. S. Morales, J. J. S. Méndez, Partition of a nonempty fuzzy set in nonempty convex fuzzy subsets, *Appl. Math. Sci.*, **6** (2012), 2917–2921.
28. M. Z. Ahmad, M. K. Hasan, B. De Baets, Analytical and numerical solutions of fuzzy differential equations, *Inform. Sciences*, **236** (2013), 156–167. https://doi.org/10.1016/j.ins.2013.02.026
29. K. Kanagarajan, M. Sambath, Runge-Kutta Nystrom method of order three for solving fuzzy differential equations, *Comput. Method. Appl. Math.*, **10** (2010), 195–203. https://doi.org/10.2478/cmam-2010-0011
30. C. Duraisamy, B. Usha, Another approach to solution of fuzzy differential equations, *Appl. Math. Sci.*, **4** (2010), 777–790.

AIMS Press